1 History and Fundamental Principles of the Diesel Engine

Klaus Mollenhauer and Klaus Schreiner

1.1 The History of the Diesel Engine

On February 27, 1892, the engineer Rudolf Diesel filed a patent with the Imperial Patent Office in Berlin for a "new rational heat engine". On February 23, 1893, he was granted the patent DRP 67207 for the "Working Method and Design for Combustion Engines" dated February 28, 1892. This was an important first step toward the goal Diesel had set himself, which, as can be gathered from his biography, had preoccupied him since his days as a university student.

Rudolf Diesel was born to German parents in Paris on March 18, 1858. Still a schoolboy when the Franco-Prussian War of 1870–1871 broke out, he departed by way of London for Augsburg where he grew up with foster parents. Without familial and financial backing, young Rudolf Diesel was compelled to take his life into his own hands and contribute to his upkeep by, among other things, giving private lessons. Scholarships ultimately enabled him to study at the Polytechnikum München, later the Technische Hochschule, from which he graduated in 1880 as the best examinee ever up to that time.

There, in Professor Linde's lectures on the theory of caloric machines, the student Diesel realized that the steam engine, the dominant heat engine of the day, wastes a tremendous amount of energy when measured against the ideal energy conversion cycle formulated by Carnot in 1824 (see Sect. 1.2). What is more, with efficiencies of approximately 3%, the boiler furnaces of the day emitted annoying smoke that seriously polluted the air.

Surviving lecture notes document that Diesel already contemplated implementing the Carnot cycle as a student, if possible by directly utilizing the energy contained in coal without steam as an intermediate medium. While working at Lindes Eismaschinen, which brought him from Paris to Berlin, he also ambitiously pursued the idea of a rational engine, hoping his invention would bring him financial independence together with social advancement. He ultimately filed and was granted the aforementioned patent [1-1] with the following claim 1:

> Working method for combustion engines characterized by pure air or another indifferent gas (or steam) with a working piston compressing pure air so intensely in a cylinder that the temperature generated as a result is far above the ignition temperature of the fuel being used (curve 1-2 of the diagram in Fig. 2), whereupon, due to the expelling piston and the expansion of the compressed air (or gas) triggered as a result (curve 2-3 of the diagram in Fig. 2), the fuel is supplied so gradually from dead center onward that combustion occurs without significantly increasing pressure and temperature, whereupon, after the supply of fuel is terminated, the mass of gas in the working cylinder expands further (curve 3-4 of the diagram in Fig. 2).

Once the gas has been decompressed to the discharge pressure, heat dissipates along the isobars 4-1 (Fig. 1-1), thus ending the cycle.

A second claim asserts patent protection of multistage compression and expansion. Diesel proposed a three cylinder compound engine (Fig. 1-2). Adiabatic compression occurs in two high pressure cylinders 2, 3 operating offset at 180° and the fuel (Diesel initially spoke of coal dust) supplied by the hopper B in top dead center auto-ignites so that isothermal combustion and expansion occur, which turns adiabatic after combustion ends. The combustion gas is transferred into the double-acting center cylinder 1 where it completely expands to ambient pressure and is expelled after the reversal of motion at the same time as the isothermal precompression by water injection or the preceding intake of the fresh charge for the second engine cycle that runs parallel. Thus, one cycle occurs per revolution.

To implement the Carnot cycle, Diesel reverted to the four-stroke cycle considered "state-of-the-art" since Nikolaus Otto's day. He believed isothermal combustion at a maximum of 800°C would enable him to keep the thermal load in the engine low enough that it would run without cooling. This limiting temperature requires compressions of approximately 250 at with which Diesel far surpassed the "state-of-the-art": On the one hand, this gave the "outsider" Diesel the naïveté

K. Mollenhauer (✉)
Berlin, Germany
e-mail: Klamoll@aol.com

K. Mollenhauer, H. Tschoeke (eds.), *Handbook of Diesel Engines*, DOI 10.1007/978-3-540-89083-6_1,

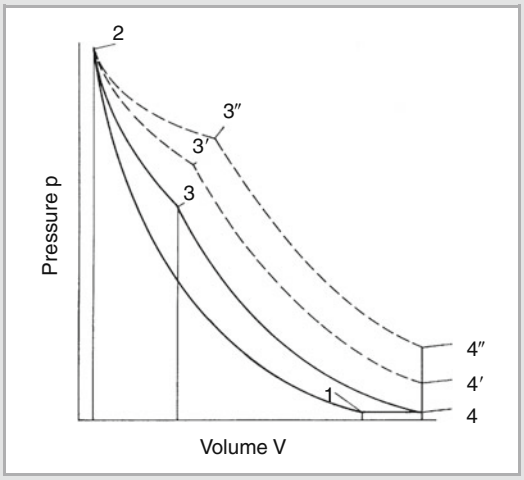

Fig. 1-1 Ideal diesel engine process (1-2-3-4) based on Fig. 2 in [1-1], supplemented by modified "admission periods" (1-2-3′-4′ and 1-2-3′′-4′′) according to Diesel's letter to Krupp of October 16, 1893 [1-4, p. 404]

necessary to implement his idea. On the other hand, firms experienced in engine manufacturing such as the Deutz gas engine factory shied away from Diesel's project.

Conscious that "an invention consists of two parts: The idea and its implementation" [1-2], Diesel wrote a treatise on the "Theory and Design of a Rational Heat Engine" [1-3] and sent it to professors and industrialists as well as Deutz at the turn of 1892–1893 to propagate his ideas and win over industry: With a Carnot efficiency of approximately 73% at 800°C, he expected maximum losses of 30 to 40% in real operation, which would correspond to a net efficiency of 50% [1-3, p. 51].

After nearly a year of efforts and strategizing, Diesel finally concluded a contract in early 1893 with the renowned Maschinenfabrik Augsburg AG headed by Heinrich Buz, a leading manufacturer of steam engines. The contract contained Diesel's concessions to an ideal engine: The maximum pressure was lowered from 250 at to 90 at and later 30 at, the compound engine's three cylinders were reduced to one high pressure cylinder and coal dust was abandoned as the fuel. Two other heavy machinery manufacturers, Krupp and, soon thereafter, Sulzer entered into the contract, which was lucrative for Diesel.

Construction of the first uncooled test engine with a stroke of 400 mm and a bore of 150 mm was begun in Augsburg early in the summer of 1893. Although petroleum was the intended fuel, gasoline was first injected in a powered engine on August 10, 1893 under the misguided assumption it would ignite more easily: The principle of auto-ignition was indeed confirmed even though the indicator burst at pressures over 80 bar!

Selected indicator diagrams (Fig. 1-3) make it possible to follow the further developments: Once the first engine, which was later provided water cooling, had been modified, the fuel could no longer be injected directly. Rather, it could only be injected, atomized and combusted with the aid of compressed air. The first time the hitherto powered engine idled on February 17, 1894, it became autonomous. Finally, a first braking test was performed on June 26, 1895: Using petroleum as fuel and externally compressed injection air, an indicated efficiency of $\eta_i = 30.8\%$ and a net efficiency of $\eta_e = 16.6\%$ were measured at a consumption of 382 g/HPh.

Only a revised design, the third test engine [1-4] furnished with a single stage air pump, delivered the breakthrough though: Professor Moritz Schröter from the Technische Hochschule München conducted acceptance tests on February 17, 1897. Together with Diesel and Buz, he presented the results at a general meeting of the Association of German Engineers in Kassel on June 16, 1897, thus introducing the first heat engine with an efficiency of 26.2%, which was sensational in those days [1-5]!

It necessitated abandoning the isothermal heat input claimed in the original patent: In light of the narrow region of the diagram proportional to indicated work and the frictional losses to be expected as a result of the high pressures, even Diesel must have realized no later than when he plotted the theoretical indicator diagrams (Fig. 1-4) that the engine would not perform any effective work. Taking great pains not to jeopardize the basic patent, he gave thought early on to prolonging the "admission period", i.e. raising the line of isothermal heat input in the p, V diagram (Fig. 1-1). A second application for a patent (DRP 82168) on November 29, 1893 also cited the constant pressure cycle, which was considered consistent with the basic patent because of its "insubstantial pressure increase". The patent granted overlooked the fact that, contrary to the basic patent, both the mass of the fuel and the maximum temperature increased!

Unsurprisingly, Diesel and the Diesel consortium were soon embroiled in patent disputes in Kassel. According to the charge, Diesel's engine did not fulfill any of his patent claims: The engine was unable to run without cooling and expansion did not occur without substantially increasing pressure and temperature as a function of compression. Only the auto-ignition mentioned in claim 1 took place. Yet, just as Diesel never admitted that his engine did not complete any phase of the Carnot cycle, he vehemently denied to the end that auto-ignition was a basic characteristic of his invention [1-4, p. 406].

The additional charge that coal dust was not employed was less weighty [1-5, 1-6]: Especially since his engine was intended to replace the steam engine, Diesel, a nineteenth century engineer, was at first unable to circumvent coal, the primary source of energy in his day. However, he did not rule out other fuels as later tests, even with vegetable oils among other things, prove [1-2]. Measured against the "state-of-the-art" of the day, nobody, not even Diesel, could have known which fuel was best suited for the Diesel engine. Documented by many draft designs, his ingeniously intuitive grasp of the

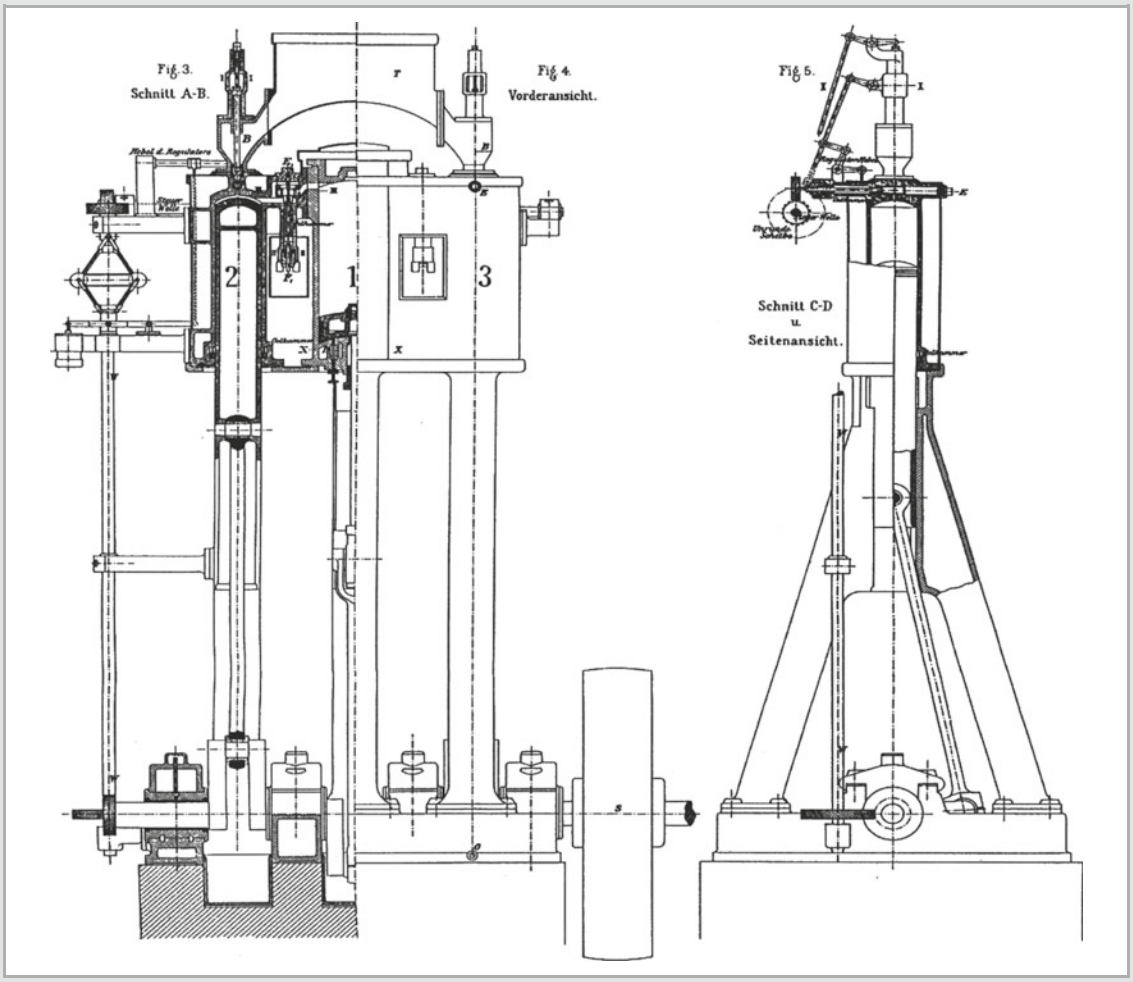

Fig. 1-2 Diesel's design of a compound engine [1-3]

diesel engine's combustion cycles, which were largely unfamiliar to him then and are often only detectable with advanced measurement and computer technology today (see Sect. 3), is all the more admirable (Fig. 1-5).

In addition to successfully weathered patent disputes, the Diesel engine's path continued to be overshadowed by conflicts between the inventor and the Diesel consortium: The latter was interested in profitably "marketing" the engine intended to replace stationary and ship steam engines as soon as possible [1-7]. First, the marketability prematurely asserted in Kassel had to be established. This was done, above all, thanks to the skill and dogged commitment of Immanuel Lauster in Augsburg. It also presaged the line of development of "high performance diesel engines" (Table 1-1).

On the other hand, principally interested in distributed energy generation [1-3, pp. 89ff] and thus anticipating cogeneration unit technology and modern developments in railroad engineering [1-8] that quite realistically envision satellite remote controlled, automatically guided boxcars [1-3], Rudolf Diesel considered the heavy test engine with its A-frame borrowed together with the crosshead engine from steam engine engineering to only be a preliminary stage on the way to a lightweight "compressorless" diesel engine.

The end of Diesel's development work at Maschinenfabrik Augsburg was marked by the reluctantly conceded construction of a compound engine unable to fulfill the hopes placed in it and a few tentative tests of coal dust and other alternative fuels.

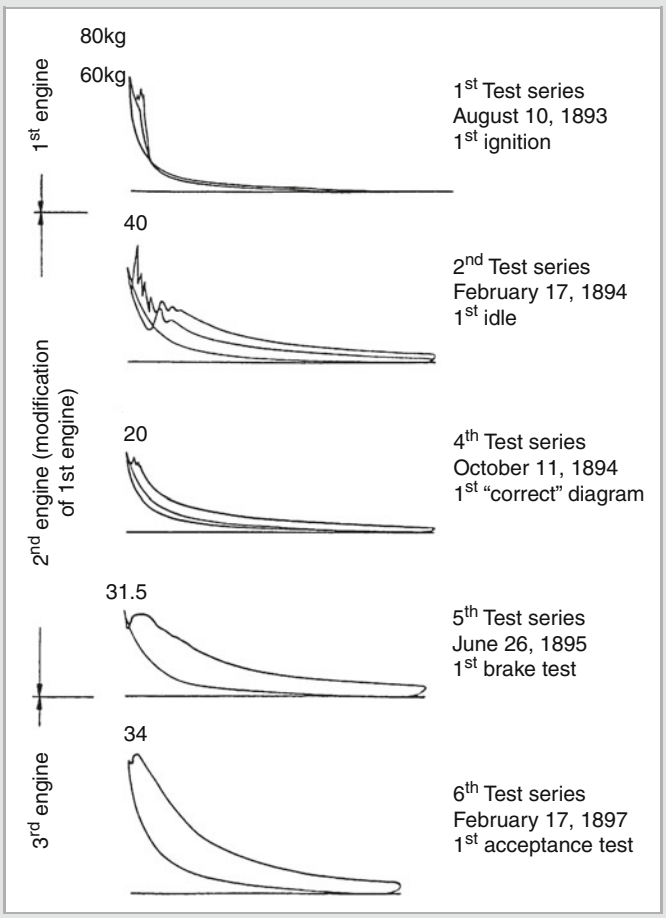

Fig. 1-3
Indicator diagrams of the evolution of the diesel engine based on [1-2]. The area enclosed by the pressure curve as a function of the cylinder volume corresponds to the engine's internal work, see Sect. 1.2

One of Diesel's later tests together with the small firm Safir intended to bring about general acceptance of the line of "vehicle diesel engine" development failed, among other things, because of the poor fuel metering. This problem was first solved by Bosch's diesel injection system [1-9].

Rudolf Diesel met his fate during a crossing from Antwerp to Harwich between September 29 and 30, 1913, just a few weeks after the appearance of his book: "The Origin of the Diesel Engine". After years of struggle and exertion had strained his mental and physical powers to their limit, financial collapse was threatening despite his vast multimillion earnings from his invention: Too proud to admit he had speculated badly and made mistakes or to accept help, Diesel, as his son and biographer relates, saw suicide as the only way out [1-10].

Left behind is his life's work, the high pressure engine that evolved from the theory of heat engines, which bears his name and, 100 years later, is still what its ingenious creator Rudolf Diesel intended: The most rational heat engine of its and even our day (Fig. 1-6). Compared to 1897, its efficiency has approximately doubled and corresponds to the approximation of Carnot efficiency estimated by Diesel. Maximum cylinder pressure p_{Zmax} has more than quintupled and, at 230 bar in present day high performance engines (MTU 8000, see Sect. 17.4), nearly achieves the maximum value Diesel proposed for the Carnot cycle at more than ten times the power density P_A.

Measured by the *ecological imperative*, the diesel engine's high efficiency and multifuel compatibility conserves limited resources and reduces environmental pollution by the greenhouse gas carbon dioxide. However, only consistent development that continues to further reduce exhaust and noise emissions will ensure the diesel engine is accepted in the future too. At the same time, it might also be possible to fulfill Diesel's vision [1-10]:

"That my engine's exhaust gases are smokeless and odorless".

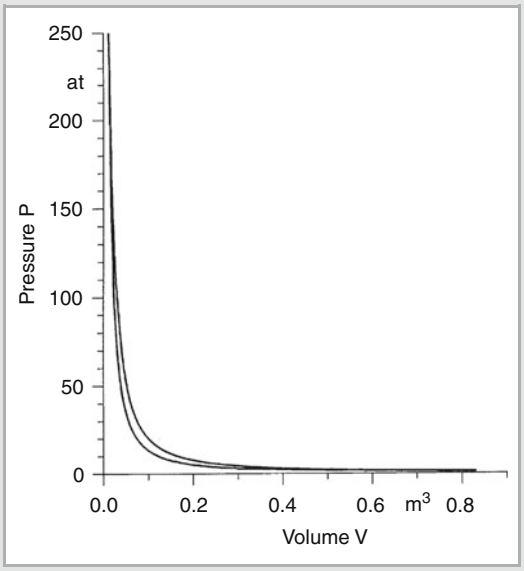

Fig. 1-4 Theoretical indicator diagrams of the Carnot cycle based on [1-3]

1.2 Fundamentals of Engine Engineering

1.2.1 Introduction

Just like gasoline engines, diesel engines are, in principle, energy converters that convert chemically bound fuel energy into mechanical energy (effective work) by supplying the heat released by combustion in an engine to a thermodynamic cycle.

As a function of the system boundaries of the converter represented as a "black box", the energy balance (Fig. 1-7) is:

$$E_B + E_L + W_e + \Sigma E_V = 0.$$

If the energy of the combustion air relative to the ambient state is $E_L = 0$, then the energy supplied with the fuel m_B is equal to the effective work W_e and the total of all energy losses ΣE_V.

The technical system of a "diesel engine" is also part of a widely networked global system defined by the concepts of "resources" and "environmental pollution". A view based purely on energy and economics aimed at minimizing the losses ΣE_V fails to satisfy present day demands specified by the ecological imperative according to which energy and material must always be converted with *maximum efficiency while minimally polluting the environment*. The outcome of the complex research and development work made necessary by these demands is the diesel engine of our day, which has evolved from a simple engine into a complex engine system consisting of a number of subsystems (Fig. 1-8). The increased integration of electrical and electronic components and the transition from open control systems to closed control loops are characteristic of this development. Moreover, international competition is making minimum manufacturing costs and material consumption imperative. Among other things, this requires fit-for-purpose designs that optimally utilize components.

1.2.2 Basic Engineering Data

Every reciprocating engine's geometry and kinematics are clearly specified by the geometric parameters of the:
- stroke/bore ratio $\zeta = s/D$,
- connecting rod ratio $\lambda_{Pl} = r/l$ and
- compression ratio $\varepsilon = V_{max}/V_{min} = (V_c + V_h)/V_c$.

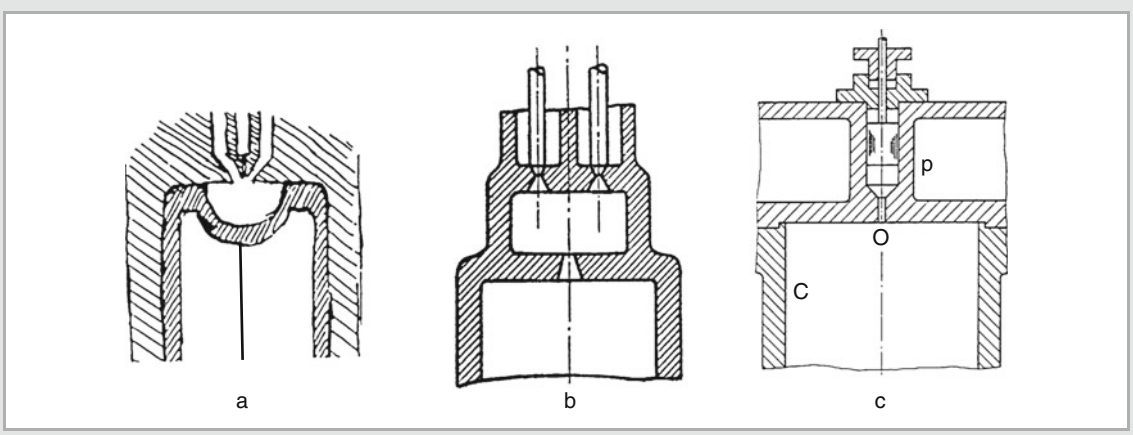

Fig. 1-5 Diesel's proposals for a combustion system. (**a**) Piston with piston crown bowl (1892); (**b**) secondary combustion chamber (1893); (**c**) Pump-nozzle unit (1905), see Sect. 5.3

Table 1-1 Milestones in the development of the diesel engine

Line of "high performance large diesel engine" development	
1897	First run of a diesel engine with an efficiency of $\eta_c = 26.2\%$ at Maschinenfabrik Augsburg
1898	Delivery of the first two-cylinder diesel engine with 2 × 30 HP at 180 rpm to the Vereinigte Zündholzfabriken AG in Kempten
1899	First two-stroke diesel engine from MAN by Hugo Güldner (unmarketable)
1899	First diesel engine without a crosshead, model *W*, from Gasmotorenfabrik Deutz
1901	First MAN trunk-piston diesel engine by Imanuel Lauster (model DM 70)
1903	First installation of a two cylinder four-stroke opposed piston diesel engine with 25 HP in a ship (the barge Petit Pierre) by Dyckhoff, Bar Le Duc
1904	First MAN diesel power station with 4 × 400 HP starts operation in Kiev
1905	Alfred Büchi proposes utilizing exhaust gas energy for supercharging
1906	Introduction of the first reversible two-stroke engine by the Sulzer and Winterthur brothers for a marine engine 100 HP/cyl. ($s/D = 250/155$)
1912	Commissioning of the first seagoing ship MS Selandia with two reversible four-stroke diesel engines from Burmeister & Wain each with 1,088 HP
1914	First test run of a double acting six-cylinder two-stroke engine with 2,000 HP/cyl. from MAN Nürnberg ($s/D = 1050/850$)
1951	First MAN four-stroke diesel engine (model 6KV30/45) with high-pressure supercharging: $\eta_{le} = 44.5\%$ at $w_{emax} = 2.05$ kJ/l, $p_{Zmax} = 142$ bar and $P_A = 3.1$ W/mm^2
1972	Hitherto largest two-stroke diesel engine ($s/D = 1{,}800/1{,}050$, 40,000 HP) commences operation
1982	Market launch of super long stroke, two-stroke engines with $s/D \approx 3$ (Sulzer, B & W)
1984	MAN B & W achieves consumption of 167.3 g/kWh ($\eta_e = 50.4\%$)
1987	Commissioning of the largest diesel-electric propulsion system with MAN-B & W four-stroke diesel engines and a total output of 95,600 kW to drive the Queen Elizabeth 2
1991/92	Two-stroke and four-stroke experimental engines from Sulzer (RTX54 with $p_{Zmax} = 180$ bar, $P_A = 8.5$ W/mm^2) and MAN B & W (4T50MX with $p_{Zmax} = 180$ bar, $P_A = 9.45$ W/mm^2)
1997	Sulzer12RTA96C (s/D = 2,500/960): two-stroke diesel engine, $P_e = 65{,}880$ kW at $n = 100$ rpm commences operation
1998	Sulzer RTX-3 research engine to test common rail technology on large two-stroke diesel engines
2000/01	MAN B & W 12K98MC-C (s/D = 2,400/980): The currently most powerful two-stroke diesel engine with $P_e = 68{,}520$ kW at $n = 104$ rpm
2004	First four-stroke medium speed diesel engine MAN B & W 32/40, $P_e = 3{,}080$ kW, common rail (CR) injection in real use on a container ship
2006	With a consumption of $b_e = 177$ g/kWh, the MaK M43C is the leading four-stroke medium speed marine engine with a cylinder output of 1,000 kW (s/D = 610/430, $w_e = 2.71$ kJ/dm^3, $c_m = 10.2$ m/s)
2006	Wärtsilä commissions the world's first 14 cylinder two-stroke engine and thus the most powerful diesel engine: Wärtsilä RTA-flex96C, CR injection, $P_e = 80{,}080$ kW, s/D = 2,500/900, $c_m = 8.5$ m/s, $w_e = 1.86$ kJ/dm^3 ($p_e = 18.6$ bar)
Line of "high-speed vehicle diesel engine" development	
1898	First run of a two cylinder four-stroke opposed piston engine ("5 HP horseless carriage engine") by Lucian Vogel at MAN Nürnberg (test engine, unmarketable)
1905	Test engine by Rudolf Diesel based on a four cylinder Saurer gasoline engine with air compressor and direct injection (unmarketable)
1906	Patent DRP 196514 by Deutz for indirect injection
1909	Basic patent DRP 230517 by L'Orange for a prechamber
1910	British patent 1059 by McKenchie on direct high pressure injection
1912	First compressorless Deutz diesel engine, model MKV, goes into mass production
1913	First diesel locomotive with four cylinder two-stroke V-engine presented by the Sulzer brothers (power 1,000 HP)
1914	First diesel-electric motor coach with Sulzer engines for the Prussian and Saxon State Railways
1924	First commercial vehicle diesel engines presented by MAN Nürnberg (direct injection) and Daimler Benz AG (indirect injection in prechamber)
1927	Start of mass production of diesel injection systems at Bosch
1931	Prototype test of the six-cylinder two-stroke opposed piston aircraft diesel engine JUMO 204 of Junkers-Motorenbau GmbH: power 530 kW (750 HP), power mass 1.0 kg/HP
1934	V8 four-stroke diesel engines with prechambers from Daimler-Benz AG for LZ 129 Hindenburg with 1,200 HP at 1,650 rpm (power mass: 1.6 kg/HP including transmission)
1936	First production car diesel engines with prechambers from Daimler-Benz AG (car model 260 D) and Hanomag
1953	First car diesel engine with swirl chamber from Borgward and Fiat
1978	First production car diesel engine with exhaust gas turbocharging (Daimler-Benz AG)
1983	First production high-speed high-performance diesel engine from MTU with twin-stage turbocharging: $w_{emax} = 2.94$ kJ/l bei $p_{Zmax} = 180$ bar, power per unit piston area $P_A = 8.3$ W/mm^2
1986/87	First ever electronic engine management (ECD) for vehicle diesel engines implemented (BMW: car, Daimler-Benz: commercial vehicle)
1988	First production car diesel engine with direct injection (Fiat)
1989	First production car diesel engine with exhaust gas turbocharging and direct injection at Audi (car Audi 100 DI)
1996	First car diesel engine with direct injection and a four-valve combustion chamber (Opel Ecotec diesel engine)
1997	First supercharged car diesel engine with direct common rail high pressure injection and variable turbine geometry (Fiat, Mercedes-Benz)

Table 1-1 (Continued)

1998	First V8 car diesel engine: BMW 3.9 l DI turbodiesel, $P_e = 180$ kW at 4,000 rpm, $M_{max} = 560$ Nm (1,750. . .2,500 rpm)
1999	Smart cdi, 0.8 dm^3 displacement, currently the smallest turbodiesel engine with intercooler and common rail high pressure injection: $P_e = 30$ kW at 4,200 rpm with 3.4 l/100 km first "3 liter car" from DaimlerChrysler
2000	First production car diesel engines with particulate filters (Peugeot)
2004	OPEL introduces a Vectra OPC study suitable for everyday with a 1.9 liter CDTI twin turbo unit with a specific power output of $P_V = 82$ kW/dm^3
2006	At the 74th 24 h Le Mans race, an AUDI R10 TDI with a V12 diesel engine ($P_e > 476$ kW at $n = 5{,}000$ rpm, $V_H = 5.5$ dm^3, $w_e = 2.1$ kJ/dm^3 with a biturbo boost pressure of $p_L = 2.94$ bar) wins the race

V_{min} corresponds to the compression volume V_c and the maximum cylinder volume V_{max} corresponds to the total from V_c and the cylinder displacement V_h, to which the following with the cylinder bore D and piston stroke s applies:

$$V_h = s \cdot \pi \cdot D^2/4.$$

Accordingly, $V_H = z \cdot V_h$ is the displacement of an engine with z cylinders.

The trunk-piston engine (Fig. 1-9) has established itself. Only large two-stroke engines (see Sect. 18.4) have a crosshead drive to relieve the piston from cornering forces (see Sect. 8.1). Both types are still only used with a unilaterally loaded piston. A standardized time value, the crank angle φ and the rotational speed ω have the following relationship:

$$\omega = d\varphi/dt = 2 \cdot \pi \cdot n.$$

When the speed n is not denoted as engine speed (s^{-1}) but rather, as is customary in engine manufacturing, in revolutions per minute (rpm), then ω is $= \pi \cdot n/30$.

An internal combustion engine's combustion cycle proceeds in the hermetic cylinder volume V_z, which changes periodically with the piston motion z_K within the boundaries V_{max} and V_{min}:

$$V_z(\varphi) = V_c + z_K(\varphi) \cdot \pi \cdot D^2/4.$$

With the crank radius r as a function of the instantaneous crank position φ in crank angle degree (°CA) and top dead center TDC ($\varphi = 0$) as the starting point, the following applies to the piston stroke:

$$z_K = r \cdot f(\varphi),$$

The following approximation function is usually applied:

$$f(\varphi) = 1 - \cos\varphi + (\lambda_{Pl}/4) \cdot \sin^2\varphi.$$

The following ensues for instantaneous piston velocity c_K and acceleration a_K:

$$c_K = dz_K/dt = r \cdot \omega \cdot [\sin\varphi + (\lambda_{Pl}/2) \cdot \sin 2\varphi]$$
$$a_K = d^2z_K/dt^2 = -r \cdot \omega \cdot [\cos\varphi + \lambda_{PL} \cdot \cos 2\varphi].$$

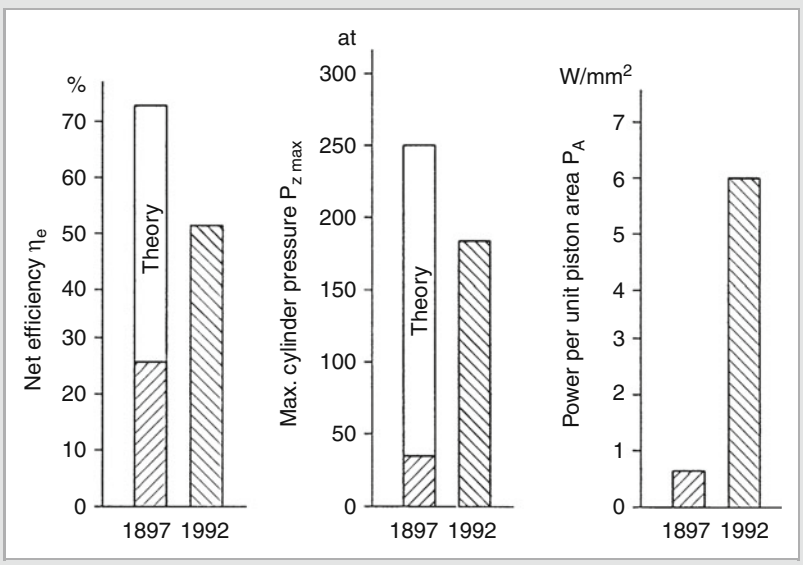

Fig. 1-6
Optimum net efficiency η_e, maximum cylinder pressure p_{Zmax} and power per unit piston area P_A for production engines approximately 100 years after the introduction of the first diesel engine (see also Fig. 1-13 and Table 1-3)

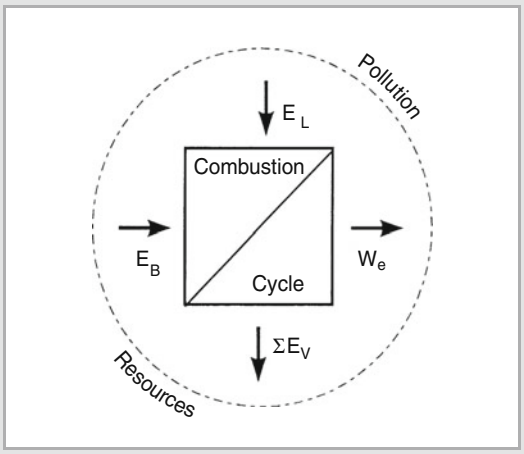

Fig. 1-7 The diesel engine as an energy converter

Following from the piston stroke s in m and engine speed n in s^{-1}, the *mean piston velocity*

$$c_m = 2 \cdot s \cdot n \quad [\mathrm{m/s}] \tag{1-1}$$

is an important *parameter for kinematic and dynamic engine performance*. As it increases, inertial forces ($\sim c^2{}_m$), friction and wear also increase. Thus, c_m may only be increased to a limited extent. Consequently, a large engine runs at low speeds or a high-speed engine has small dimensions. The following correlation to engine size is approximated for diesel engines with a bore diameter of $0.1\ m < D < 1$ m:

$$c_m \approx 8 \cdot D^{-1/4}. \tag{1-2}$$

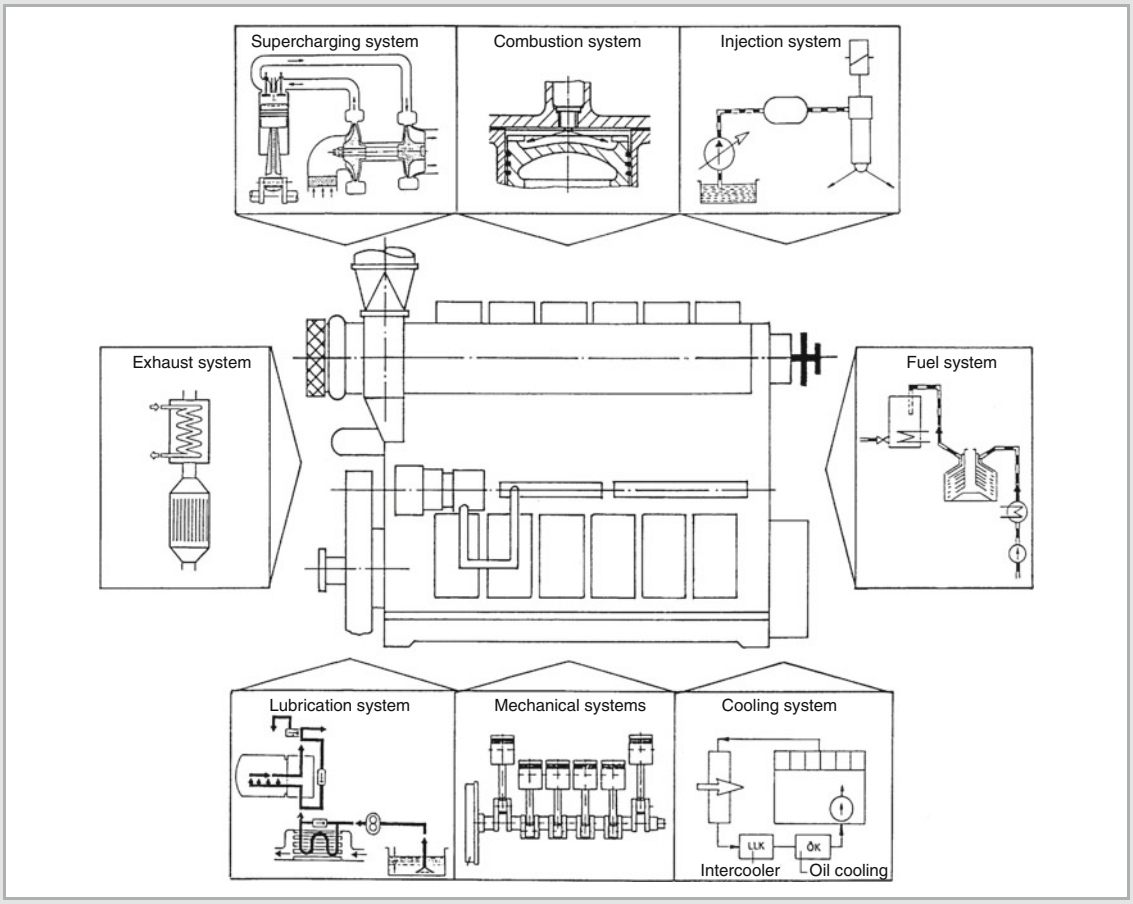

Fig. 1-8 The modern diesel engine as a complex of subsystems

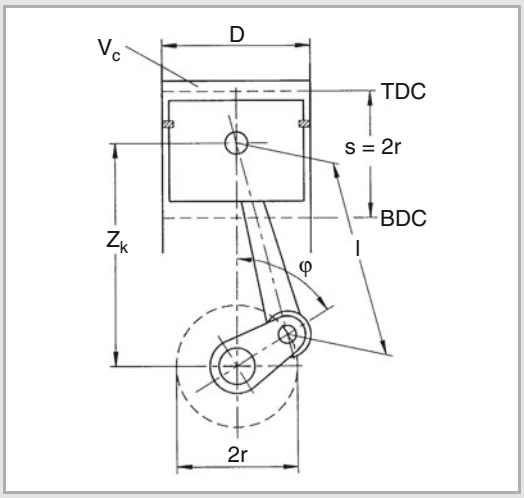

Fig. 1-9 Basic engineering data of a trunk-piston engine

1.2.3 Engine Combustion

1.2.3.1 Fundamentals of Combustion Simulation

Chemically, combustion is the oxidation of fuel molecules with atmospheric oxygen as the oxidant. Thus, the maximum convertible fuel mass m_B is limited by the air mass present in the engine cylinder. Using the fuel-specific stoichiometric air requirement L_{min} (kg air/kg fuel) for complete combustion, the air/fuel ratio λ_V specifies the ratio of "supply to demand" in combustion:

$$\lambda_v = m_{LZ}/(m_B \cdot L_{min}). \quad (1\text{-}3)$$

The following applies to the "supply" of the air mass m_{LZ} of all cylinders ($V_Z = z \cdot V_z$) contained in the entire engine:

$$m_{LZ} = V_Z \cdot \rho_Z = \lambda_l \cdot \rho_L \cdot V_H. \quad (1\text{-}4)$$

Since the density ρ_Z of the cylinder charge is usually unknown, the definitions of the volumetric efficiency λ_l (see Sect. 2.1) and the density ρ_L of the fresh charge directly at the inlet to the cylinder head are generally reverted to:

$$\rho_L = p_L/(R_L \cdot T_L). \quad (1\text{-}5)$$

The air requirement ensues from the elemental analysis of the fuel: A petroleum derivative, diesel fuel (DF) is a conglomerate of hydrocarbons and primarily consists of carbon C, hydrogen H and sulfur S with usually insignificant fractions of oxygen O and nitrogen N. Thus, the balance equation for the complete oxidation of a generic fuel molecule $C_xH_yS_z$ into carbon dioxide CO_2, water H_2O and sulfur dioxide SO_2

$$C_xH_yS_Z + [x + (y/2) + z] \cdot O_2 \rightarrow$$
$$x \cdot CO_2 + (y/2) \cdot H_2O + z \cdot SO_2 + Q_{ex},$$

yields the stoichiometric air/fuel ratio L_{min} corresponding to the oxygen content of the air and the particular number of moles:

$$L_{min} = 11.48 \cdot (c + 2.98 \cdot h) + 4.3 \cdot s - 4.31 \cdot o \ [kg/kg]$$

(c, h, s, o: mass fraction of 1 kg fuel according to the elemental analysis. Reference value for DK: $L_{min} = 14.5$ kg/kg).

The heat Q_{ex} released during combustion corresponds to the fuel-specific *calorific value* H_u, which may also be calculated [1-11] from the elemental analysis as:

$$H_u = 35.2 \cdot c + 94.2 \cdot h + 10.5 \cdot (s - o) \quad [MJ/kg]$$

The following approximate relation is based on the fuel density ρ_B at 15°C:

$$H_u = 46.22 - 9.13 \cdot \rho_B^2 + 3.68\rho_B \quad [MJ/kg].$$

Thus, the following applies to the heat supplied to the combustion cycle by "internal combustion":

$$E_B = Q_{zu} \leq m_B \cdot H_u.$$

1.2.3.2 Comparison of Engine Combustion Systems

Combustion is preceded by the preparation of usually liquid fuel to obtain a combustible mixture of fuel vapor and air. This process proceeds differently in diesel and gasoline engines (Table 1-2).

Internal mixture formation in diesel engines (see Chap. 3) begins with the injection of the fuel into the highly compressed and thus heated air shortly before TDC, whereas *external mixture* in classic gasoline engines is formed outside the working chamber by a carburetor or by injection into the intake manifold and often extends through the induction and compression stroke.

While gasoline engines have a *homogeneous fuel/air mixture*, diesel engines have a *heterogeneous mixture* before ignition, which consists of fuel droplets with diameters of a few micrometers distributed throughout the combustion chamber. They are partly liquid and partly surrounded by a fuel vapor/air mixture.

Provided the *air/fuel ratio* of the homogeneous mixture lies within the ignition limits, combustion in gasoline engines is triggered by controlled spark ignition by activating an electrical discharge in a spark plug. In diesel engines, already prepared droplets, i.e. droplets surrounded by a combustible mixture, *auto-ignite*. Ignition limits in the stoichiometric mixture range ($\lambda_V = 1$) only exist for the micromixture in the region of the fuel droplets (see Chap. 3).

Table 1-2 Comparison of features of engine combustion

Feature	Diesel engine	Gasoline engine
Mixture formation	Inside V_z	Outside V_z
Type of mixture	Heterogeneous	Homogenous
Ignition	Auto-ignition with excess air	Spark ignition within ignition limits
Air/fuel ratio	$\lambda_V \geq \lambda_{min} > 1$	$0.6 < \lambda_V < 1.3$
Combustion	Diffusion flame	Premix flame
Torque change through fuel	Variable l_V (quality control) Highly ignitable	Variable mixture quantity (quantity control) Ignition resistant

Diesel engines require excess air ($\lambda_V \geq \lambda_{min} > 1$) for normal combustion. Consequently, the *supply of energy is adapted to the engine load* in diesel engines by the air/fuel ratio, i.e. the *mixture quality* (quality control) and, in light of the ignition limits, by the *mixture quantity* (quantity control) in gasoline engines by throttling that entails heavy losses when a fresh charge is aspirated.

The type of ignition and mixture formation determines the *fuel requirements*: Diesel fuel must be *highly ignitable*. This is expressed by its *cetane number*. Gasoline must be *ignition resistant*, i.e. have a high *octane number*, so that uncontrolled auto-ignition does not trigger uncontrolled combustion (detonation). The latter is ensured by low boiling, short chain and thus thermally stable hydrocarbons (C_5 through C_{10}). Diesel fuel, on the other hand, consists of high boiling, long chain hydrocarbons (C_9 through C_{30}) that disintegrate earlier and form free radicals that facilitate auto-ignition (see Chap. 3).

1.2.4 Fundamentals of Thermodynamics

1.2.4.1 Ideal Changes of States of Gases

The state of a gas mass m is determinable by two thermal state variables by using the general equation of state for ideal gases:

$$p \cdot V = m \cdot R \cdot T$$

(p absolute pressure in Pa, T temperature in K, V volume in m^3, R specific gas constant, e.g. for air $R_L = 287.04$ J/kg · K). Ideal gases are characterized by a constant isentropic exponent κ (air: $\kappa = 1.4$; exhaust gas: $\kappa \approx 1.36$) as a function of pressure, temperature and gas composition.

Consequently, the state of a gas can be represented in a p, V diagram with the variables p and V and tracked. Changes of state are easy to calculate by setting constants of a state variable for which simple closed equations exist for isobars (p = const.), isotherms (T = const.) and isochors (V = const.) [1-12]. The adiabatic change of state is a special case:

$$p \cdot V^{\kappa} = \text{const.},$$

heat not being transferred between the gas and the environment. When this cycle is reversible, it is called an isentropic change of state. However, just as the real isentropic exponent depends on the state and composition of a gas, this is never actually the case in reality [1-13].

1.2.4.2 Ideal Cycle and Standard Cycle

In an ideal cycle, the gas undergoes a self-contained change of state, returning to its initial state once it has completed the cycle. Thus, the following applies to the internal energy $U = U(T)$:

$$\oint \mathrm{d}U = 0.$$

Hence, from the first law of thermodynamics that describes the conservation of energy in closed systems:

$$\partial Q = \mathrm{d}U + p \cdot \mathrm{d}V,$$

it follows that the heat Q converted during the cycle accumulates as mechanical work:

$$\oint \partial Q = \oint p \cdot \mathrm{d}V = W_{th},$$

i.e. the change in pressure and volume corresponds to the theoretically useful work W_{th} of the ideal cycle.

An ideal cycle becomes the standard cycle for a thermal machine once it has been adjusted for reality. For a reciprocating piston engine, this means that the ideal cycle and real combustion cycle proceed similarly between two volume and pressure limits specified by V_{max} and V_{min} and p_{max} and p_{min}. The upper pressure limit p_{max} corresponds to the maximum cylinder pressure p_{Zmax} allowable for reasons of stability and p_{min} the air pressure p_L before intake into the engine (Fig. 1-10a). Other specifications that must agree are the compression ratio ε and input heat Q_{zu} or Q_B:

$$Q_{zu} = Q_B = m_B \cdot H_u.$$

When the mass of the fresh charge m_{LZ} is given (Eq. (1-4)), the fuel mass m_B is limited by the air/fuel ratio λ_V and the *calorific value of the mixture* h_u:

$$h_u = Q_{zu}/(m_B + m_{LZ}) = H_u/(1 + \lambda_v \cdot L_{min}).$$

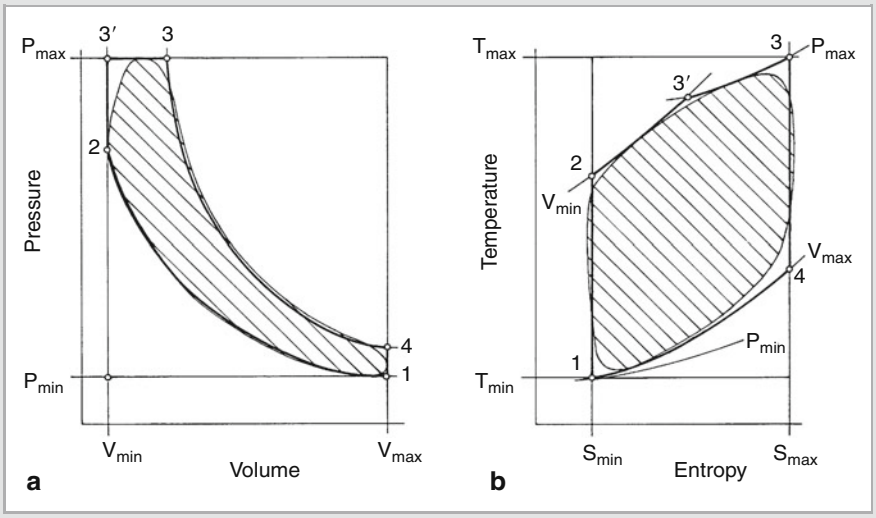

Fig. 1-10
The Seiliger cycle as standard cycle for internal combustion engines in a p, V diagram (**a**) and T, s diagram (**b**)

Based on the diesel engine's combustion phase and assuming the gas exchange phase is free of losses along the isobars $p_{\min}$ (see Sect. 2.1), the standard cycle in 1 begins with adiabatic compression to $p_2 = p_c = p_1 \cdot \varepsilon^{\kappa}$ (Fig. 1-10a). Afterward, heat is transferred: first, isochorically until it reaches the limit pressure $p_{\max}$ in 3′ and, then, isobarically up to 3. The adiabatic expansion that follows ends in 4. The cycle concludes when heat begins to dissipate along the isochors $V_{\max}$ afterward. The area of the region 1-2-3′-3-4-1 corresponds to the theoretical work:

$$W_{\text{th}} = h_{\text{th}} \cdot Q_{\text{zu}},$$

Applying the charging ratio $\delta = V_3/V_2$ and the pressure ratio $\psi = p_3/p_2$ makes it possible to specify a closed expression (provided that $\kappa = \text{const.}$) for the thermal efficiency η_{th} of the Seiliger cycle described here

$$\eta_{\text{th}} = (1 - \varepsilon^{1-\kappa}) \cdot (\delta^{\kappa} \cdot \psi - 1)/[\psi = 1 + \kappa \cdot (\delta - 1)],$$

The Seiliger cycle's conversion of energy can be followed in the temperature entropy (T, s-) diagram (Fig. 1-10b): Since the areas of the regions $s_{\min}$-1-2-3′-3-4-$s_{\max}$ and $s_{\min}$-1-4-$s_{\max}$ correspond to the heat supplied Q_{zu} and extracted Q_{ab} respectively, the difference corresponds to the theoretical effective work. Thus, the following applies to thermal efficiency:

$$\eta_{\text{th}} = (Q_{\text{zu}} - Q_{\text{ab}})/Q_{\text{zu}} = W_{\text{th}}/Q_{\text{zu}}. \qquad (1\text{-}6)$$

The rectangles formed by the limit values in both diagrams correspond to the maximum useful work in each case, yet with different efficiencies: The full load diagram of an ideal reciprocating piston steam engine with moderate efficiency in the p, V diagram is presented alongside the Carnot efficiency with real non-useable work (see Sect. 1.1). The temperature difference $T_{\max} - T_{\min}$ is crucial to the Carnot cycle's efficiency η_c:

$$\eta_c = (T_{\max} - T_{\min})/T_{\max}.$$

The T, s diagram reveals that high temperatures (up to 2,500 K) occur even during real combustion (see Sect. 1.3). Since combustion is intermittent, the engine components fall below the temperatures critical for them when they have been designed appropriately (see Sect. 9.1). The lowest possible temperature $T_{\min} \leq T_{\text{L}}$ is also conducive to this.

Since it can be adapted to the real engine process, the Seiliger cycle corresponds to the most general case of a standard cycle. It also encompasses the limit cases of the constant volume cycle ($\delta \rightarrow 1$) and the constant pressure cycle ($\psi \rightarrow 1$), which are often referred to as the ideal gasoline engine or diesel engine process even though combustion in gasoline engines does not occur with an infinitely high combustion rate and combustion in diesel engines is not isobar (Fig. 1-11).

Allowing for the real gas behavior, i.e. $\kappa \neq const.$, the compression ratio's influence on the thermal efficiency η^{*}_{th} for a pressure ratio $p_{\max}/p_{\min} = 60$ is evident in Fig. 1-12: The allowable maximum pressure in the constant volume cycle is already exceeded for $\varepsilon \approx 9$ at an air/fuel ratio of $\lambda_{\text{V}} = 2$. A Seiliger cycle allows higher compression ratios but transforms into a constant pressure cycle for $\varepsilon \approx 19.7$.

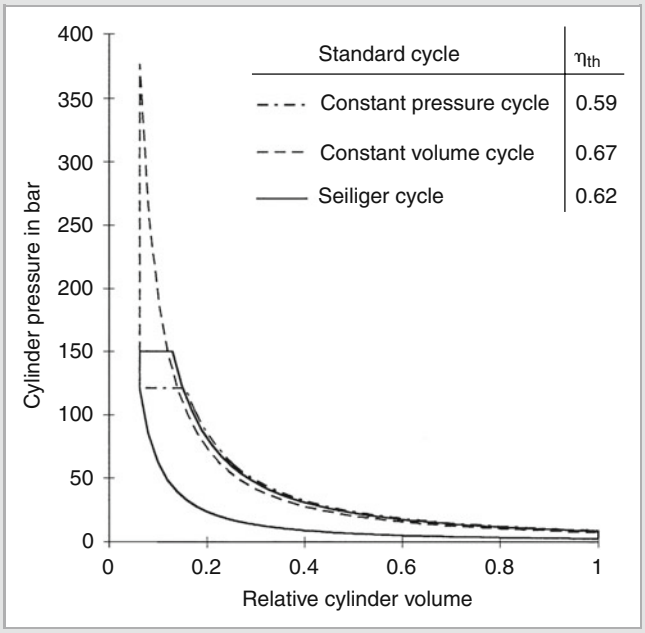

Fig. 1-11
Ideal cycle as standard cycle: Seiliger cycle ($p_{Zmax} = 150$ bar), constant pressure and constant volume cycle for $p_1 = 2.5$ bar, $T_1 = 40°C$, $\varepsilon = 16$, $\lambda_v = 2$ and $H_u = 43$ MJ/kg

Engine process simulation (Sect. 1.3) has eliminated the idealized standard cycle in the field, yet has retained its worth for quick "upward" estimates, e.g. when engine process control is varied.

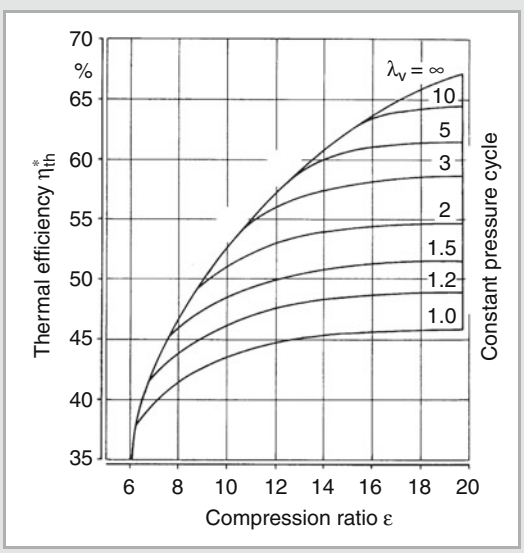

Fig. 1-12 Thermal efficiency η^*_{th} incorporating real gas behavior (based on [1-13])

1.2.5 The Diesel Engine Process

1.2.5.1 Two-stroke and Four-stroke Cycle

Unlike the idealized cycle with external heat input, internal combustion requires the exchange of the charge after every combustion phase by a gas exchange phase (see Sect. 2.1). To do so, a four-stroke engine requires two additional strokes or cycles as the motion from one dead center to the other is termed. Hence, by expelling the exhaust gas and aspirating the fresh charge after the expansion stroke (compression as well as combustion and expansion), the entire working cycle is comprised of two revolutions or 720°CA. Consequently, a frequency ratio exists between the speed and the working cycle frequency n_a:

$$a = n/n_a, \tag{1-7}$$

which is often denoted as the "cycle rate" without specifying the actual number of cycles with $a = 2$ (four-stroke cycle) or $a = 1$ (two-stroke cycle).

1.2.5.2 Real Engine Efficiencies

Along with the thermal efficiency, which enables an upward estimate, the net efficiency is of prime interest:

$$\eta_e = W_e/(m_B \cdot H_u) = \eta_{th} \cdot \eta_u \cdot \eta_g \cdot \eta_m = \eta_i \cdot \eta_m, \tag{1-8}$$

It can also be specified as the product of the thermal efficiency and the reference variable that describes the percentage loss.

Losses by incomplete combustion are included by the conversion factor:

$$\eta_u = Q_{zu}/(m_B \cdot H_u).$$

The efficiency factor:

$$\eta_g = W_i/W_{th}$$

describes the real cycle's deviations from the ideal cycle by employing
- a real instead of an ideal working gas,
- wall heat losses instead of the adiabatic change of state,
- real combustion instead of idealized heat input and
- gas exchange (throttling, heating and scavenging losses).

In accordance with DIN 1940, mechanical efficiency

$$\eta_m = W_e/W_i$$

encompasses the frictional losses at the piston and in the bearings, the heat loss of all the assemblies necessary for engine operation and the aerodynamic and hydraulic losses in the crankshaft assembly.

Referred to as indication, measurement of the cylinder head pressure curve can be used to determine the indicated work W_i (the hatched area in Fig. 1-10a) present in a piston and thus the internal (indicated) efficiency

$$\eta_i = W_i/(m_B \cdot H_u) = \oint p_z \cdot dV/(m_B \cdot H_u).$$

1.2.5.3 Engine Operation and Engine Parameters

Effective Brake Work and Torque

The effective brake work W_e ensues from the torque M and the "cycle rate" a measurable at the engine's output shaft:

$$W_e = 2 \cdot \pi \cdot a \cdot M = w_e \cdot V_H. \quad (1\text{-}9)$$

When W_e is related to displacement V_H, then the *specific work* w_e *in* kJ/dm^3 denotes the effective work obtained from one liter of displacement. Thus, along with the *mean piston velocity* c_m Eq. (1-1), it is the most important engine parameter that characterizes the "state-of-the-art". Engine companies with a sense of tradition often still apply the parameter p_e, "brake mean effective pressure", which, despite being specified in "bar", does not correspond to any *measurable pressure*. Rather, it is rooted in the history of mechanical engineering.[1] The following applies to conversions:

1 bar "brake mean effective pressure" = 0.1 kJ/dm^3.

[1] The inability to reach a consensus among the many authors from industry and academia must be borne in mind in the individual sections, especially when numerical data is provided.

Based on Eq. (1-9) with $M/V_H = w_e/(2 \cdot \pi \cdot \alpha)$, the term volume-specific torque M/V_H in Nm/dm^3 sometimes employed for vehicle engines likewise equals the specific effective work, $w_e \approx 0.0125 \cdot (M/V_H)$ applying to four-stroke engines.

Fundamental Diesel Engine Equation

With the net efficiency η_e and the air/fuel ratio λ_V, Eq. (1-8), (1-3), the following ensues for the effective work:

$$W_e = \eta_e \cdot m_B \cdot H_u = \eta_e \cdot m_{LZ} \cdot H_u/(\lambda_V \cdot L_{min}). \quad (1\text{-}10)$$

The fresh air mass m_{LZ} in an engine, Eq. (1-4), is defined by the volumetric efficiency λ_l and charge density ρ_L, Eq. (1-5), so that the following ensues for the specific effective work:

$$w_e = \eta_e \cdot \lambda_l \cdot (p_L/(R_L \cdot T_L)) \cdot (H_u/(\lambda_V \cdot L_{min})). \quad (1\text{-}11)$$

If the specific fuel parameters are regarded as given just like the indirectly influenceable efficiency, then only increasing the pressure p_L by compression, e.g. by exhaust gas turbocharging with intercooling (see Sect. 2.2), remains a freely selectable option to increase effective work since limits exist for both the volumetric efficiency with $(\lambda_l)_{max} \rightarrow \varepsilon/(\varepsilon-1)$ and the air/fuel ratio $\lambda_V \rightarrow \lambda_{min} > 1$.

Engine Power

The combustion cycle frequency n_a and specific effective work w_e, Eq. (1-7), (1-9), yield the following for the net power:

$$P_e = W_e \cdot n_a = w_e \cdot z \cdot V_h \cdot n/a, \quad (1\text{-}12)$$

and the following with the mean piston velocity c_m, Eq. (1-1):

$$P_e = C_o \cdot w_e \cdot C_m \cdot z \cdot D^2 \quad (1\text{-}13)$$

($C_0 = \pi/(8 \cdot a) \approx 0.2$ or 0.4 for four and two-stroke respectively).
With its quadratic dependence on bore diameter D, the second form of the power equation suggests a large engine is another option to boost power. At the same time, engine torque (Eq. (1-9)) increases:

$$M \sim W_e \sim w_e \cdot z \cdot D^3.$$

Accordingly, when the cylinder dimensions are retained, comparable engine power through specific work w_e can only be achieved by maximum supercharging (see Sect. 17.4).

When speed is specified in rpm, displacement in dm^3 and specific work in kJ/dm^3, the following is obtained for practical calculations

$$P_e = w_e \cdot z \cdot V_h \cdot n/(60.a)$$

or, using the brake mean effective pressure p_e in bar, the following

$$P_e = p_e \cdot z \cdot V_h \cdot n/(600.a)$$

in kW in each case.

The *fundamental diesel engine equation*, Eq. (1-11), reveals that engine power is a function of the ambient condition: A diesel engine run at an altitude of 1,000 m cannot produce the same power as at sea level. Hence, set reference conditions (x) for performance comparisons and acceptance tests for users' specific concerns have been defined to convert the power P measured into the power P_x applicable to the reference condition.[2] Generally, the following applies:

$$P_x \cong \alpha^{\beta} \cdot P.$$

In addition to air pressure and temperature, influencing variables for α and β are relative humidity, coolant inlet temperature in the intercooler and engine mechanical efficiency ($\eta_m = 0.8$ if unknown). Since a danger of overcompensation has been proven to often exist, some vehicle engine manufacturers have switched to measuring power in air conditioned test benches with ambient conditions that conform to standards. Since diesel engines have low overload capacity, the *blocked ISO net power* that may not be exceeded or the *ISO standard power* that may be exceeded depending on the engines' use is specified with the defined magnitude and duration of their extra power [1-14]. At 10% overload, it corresponds to the CIMAC recommendation for "continuous brake power" for marine engines.

Power-Related Engine Parameters

Frequently applied to vehicle engines, the displacement specific power output

$$P_V = P_e/V_H = w_e \cdot n/a. \quad (1\text{-}14)$$

is a function of the speed and thus also engine size. On the other hand, the specific power per unit piston area:

$$P_A = P_e/(z \cdot A_k) = w_e \cdot c_m/(2 \cdot a), \quad (1\text{-}15)$$

(with w_e in kJ/dm^3, c_m in m/s, $2 \cdot a = 4$ results for a four-stroke engine and $2 \cdot a = 2$ for a two-stroke engine, where P_A is in W/mm^2) is independent of engine size if the correlation from Eq. (1-2) is disregarded this once. The product of *mechanical and thermal* (w_e) as well as *dynamic load* (c_m) characterizes the "state-of-the-art" for two-stroke or four-stroke engines and large or vehicle engines in equal measure as the following example makes clear:

In a comparison of two production engines, the low speed two-stroke Wärtsilä RT96C diesel engine [1-15] with an MCR cylinder output of 5,720 kW, specific effective work of $w_e = 1.86$ kJ/dm^3 and a mean piston velocity of $c_m = 8.5$ m/s and the currently most powerful BMW diesel engine for cars (BMW 306 D4: $w_e = 1.91$ kJ/dm^3, $c_m = 13.2$ m/s [1-16]), the following ensues for the power per unit piston area and displacement specific power output:

- Wärtsilä $P_A = 7.91$ W/mm^2 and $P_V = 3.16$ kW/dm^3,
- BMW $P_A = 6.31$ W/mm^2 and $P_V = 70.2$ kW/dm^3.

The comparison of the powers per unit piston area clearly demonstrates that even the low speed two-stroke engine, sometimes derogatorily called a "dinosaur", is a "high-tech" product that even leaves the BMW 306 D4, a "powerhouse" with 210 kW rated power, far behind.[3]

A car diesel engine has to deliver its full load power on the road only very rarely, whereas a marine diesel engine – barring a few maneuvers – always runs under full load, not infrequently up to 8,000 h a year.

The development of the variable P_A presented in Fig. 1-13 reveals that the potential for diesel engine development has apparently not been exhausted yet! However, current emphases of development are geared less toward enhancing performance than reducing fuel consumption and improving exhaust emission in light of rising fuel prices.

Specific Fuel Consumption

The fuel mass flow $\dot{m}_B$ yields the performance-related specific fuel delivery rate or fuel consumption:

$$b_e = \dot{m}_B/P_e = 1/(\eta_e \cdot H_u).$$

Accordingly, comparative analyses require identical calorific values or fuels. When alternative fuels are used (see Sect. 4.2), the quality of energy conversion cannot be inferred from consumption data. Thus the specification of net efficiency is fundamentally preferable. Standard ISO fuel consumptions relate to a fuel (DF) with $H_u = 42$ MJ/kg. This allows the following conversion for specifications of fuel consumption in g/kWh:

$$\eta_e = 85.7/b_e \quad \text{and} \quad b_e = 85.7/\eta_e.$$

Specific Air Flow Rate or Air Consumption

Analogous to specific consumption, the total air flow rate $\dot{m}_L$ (see Sect. 2.1.1) yields an engine's specific air flow rate or consumption (see Table 1-3):

$$l_e = \dot{m}_L/P_e,$$

Thus, the following applies to the total air/fuel ratio:

$$\lambda = l_e/(b_e \cdot L_{min}).$$

[2] Common standards include Part 1 of DIN ISO 3046, DIN 70020 (11/76) specifically for motor vehicle engines and ECE Regulation 120 for "internal combustion engines to be installed in agricultural and forestry tractors and in non-road mobile machinery".

[3] Occasionally applied, the term "$p_e \cdot c_m$" [1-17] yields 158 (bar · m/s) for the low speed engine and 252 (bar · m/s) for the BMW engine. Since the different working processes are disregarded, the product "$p_e \cdot c_m$" is not a real variable. Moreover, the specification in (bar · m/s) defies any sound analysis.

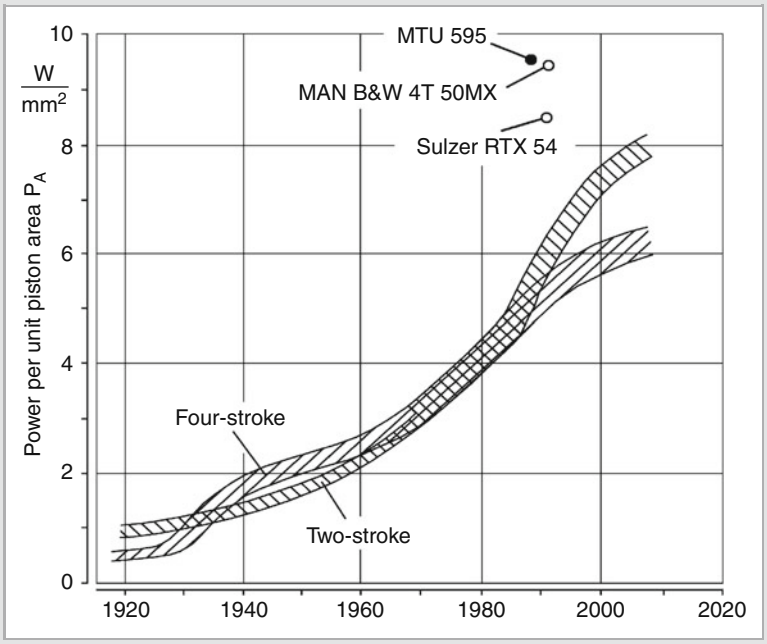

Fig. 1-13
Development of the power per unit piston area P_A of large diesel engines; maximum values of two-stroke (Sulzer RTX54) and four-stroke (MAN B&W 4T 50MX) experimental engines and a production engine (MTU 595)

Engine Characteristic Map

As a rule, the use of an engine to drive stationary systems or vehicles requires adjusting the engine characteristic map of the curve of torque M as a function of speed: As full load torque is approached, the air/fuel ratio λ_V drops so that the smoke limit is reached at $\lambda_V \rightarrow \lambda_{min}$. This corresponds to a smoke number still considered acceptable. As the speed limits n_A and n_N (starting and rated speed) increasingly spread, vehicle engines exibit a spike in the average speed range, which gives them far more flexible responsiveness (Fig. 1-14).

Table 1-3 Operating values of diesel engines at nominal load

Engine type	Specific fuel consumption b_e [g/kWh]	Spec. flow rate l_e [kg/kWh]	Air/fuel ratio λ_V	Specific oil consumption $b_{\ddot{o}}$ [g/kWh]	Exhaust gas temperature T_A after turbine [°C]
Car diesel engines:					
- without supercharging	265	4.8	1.2	<0.6	710
- with exhaust gas turbocharging	260	5.4	1.4	<0.6	650
Commercial vehicle diesel engines* with exhaust gas turbocharging and intercooling	205	5.0	1.6	<0.2	550
High performance diesel engines	195	5.9	1.8	<0.5	450
Medium speed four-stroke diesel engines	180	7.2	2.2	0.6	320
Low speed two-stroke diesel engines	170	8.0	2.1	1.1	275

* for heavy commercial vehicles and buses.
Note: While the specific air flow rate l_e not only includes the combustion air but also the scavenging air, the combustion air ratio λ_V, only incorporates the mass of the combustion air. The specified mean values cover a range of approximately ± 5%.

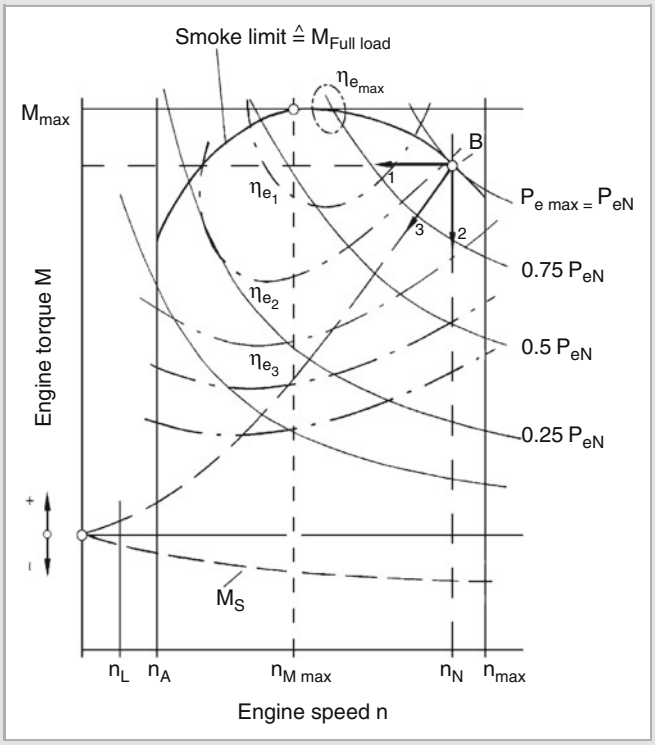

Fig. 1-14
Map representation of engine torque M with lines P_e = const. and η_e = const. and specification of selected engine characteristic maps. *1* speed decrease at rated engine torque, *2* generator operation and *3* propeller curve

Apart from the smoke limit and the power hyperbolae (curves of constant power), such engine maps also often include curves of constant efficiency and specific fuel consumption or other engine parameters. Some specific engine characteristic maps are:

1. speed decrease at rated engine torque: M = const. and n = variable,
2. generator operation: M = variable and n = const.,
3. propeller operation: $M \sim n^2$.

Depending on the rolling resistance, the entire map range can be covered for the vehicle drive including motored operation with drag torque M_s. "Speed decrease at rated engine torque" ought to be avoided in supercharged engines, since the decreasing air/fuel ratio can cause thermal overloading in limit loaded engines (see Sect. 2.2).

Corresponding to the engine characteristic map specified by the rolling resistance curves, the vehicle drive requires an adjustment of the characteristic map by converting the torque with a transmission system (Fig. 1-15). The map is limited by the maximum transferrable torque M_{Rmax} at the gear wheel ("slip limit"), the maximum engine or gear wheel speed n_{R} and the torque characteristic for $P_{\max}$ = const. denoted as the "ideal traction hyperbola". The following applies to the torque M_R acting on the gear wheel incorporating the reduction i_{ges} (gear stage, axel drive and differential) and all mechanical losses with η_{ges}:

$$M_{\mathrm{R}} = i_{\mathrm{ges}} \cdot \eta_{\mathrm{ges}} \cdot M.$$

At a running speed of $c_{\mathrm{F}} = 2 \cdot \pi \cdot R \cdot n_{\mathrm{R}}$, the following applies to driving performance that overcomes all rolling resistance ΣF_{W}:

$$P_{\mathrm{R}} = 2 \cdot \pi \cdot n_{\mathrm{R}} \cdot M_{\mathrm{R}} = C_{\mathrm{F}} \cdot \Sigma F_{\mathrm{W}}.$$

Transmission design matched to the consumption map (Fig. 1-14) can achieve favorable fuel consumption with good driving comfort (see Sect. 17.1).

1.3 Combustion Cycle Simulation

1.3.1 Introduction

The processes in a diesel engine cylinder run intensely transiently since the working cycles of compression, combustion, expansion and charge follow one another in fractions of a second. Hence, it is impossible to use the simple means of the ideal standard cycle to simulate a diesel engine accurately

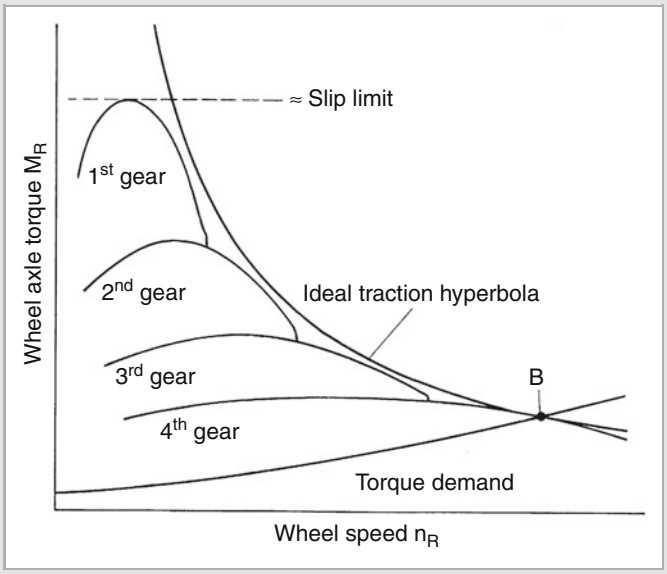

Fig. 1-15
Engine characteristic maps for a vehicle engine with four-speed transmission

enough for engine development. Rather, the differential equations of mass and energy conservation must be solved mathematically, incorporating thermal and calorific state equations.

The rapid development of data processing made it possible to solve these differential equations mathematically for the first time in the 1960s [1-18]. Since the mathematical work helped reduce high test bench costs, the first tests were performed in the large engine industry.

In the meantime, combustion cycle simulation has become a standard tool in engine development and will continue to gain importance in the future [1-19]. Applications range from simple descriptions of the processes in a cylinder up through the complex, transient processes for transient additional loading of diesel engines with two-stage sequential turbocharging allowing for dynamic user behavior [1-20–1-22].

Thermodynamic analysis of the cylinder pressure curve constitutes state-of-the-art testing today, Thanks to advanced computers, it is not only able to ascertain the instantaneous combustion characteristic but also other operating parameters such as the residual exhaust gas in a cylinder in real time [1-23]. This can be built upon for control based on cylinder pressure for new combustion systems, e.g. the HCCI system, for use in mass production, provided accurate and stable pressure sensors are available.

Naturally, an introduction to engine process simulation cannot treat every thermodynamically interesting engine assembly such as the cylinder, exhaust gas turbocharger or air and exhaust manifold systems. Hence, taking modeled thermodynamic processes in a cylinder without a divided combustion chamber as an example, the following sections only explain the fundamentals of engine process simulation. The individual sections provide references to more detailed literature.

1.3.2 Thermodynamic Foundations of Engine Process Simulation

1.3.2.1 General Assumptions

Thermodynamic Cylinder Model

The assumptions put forth in Sect. 1.2 to analyze the ideal combustion cycle can no longer be retained by engine process simulation that simulates the change of state of the cylinder charge (pressure, temperature, mass, composition, etc.) during a combustion cycle. Suitable thermodynamic models must be defined for both the individual cylinder and the process boundary conditions such as energy release by combustion, wall heat losses or the conditions before and after the cylinder (Table 1-4).

System boundaries are set for the cylinder's working chamber (Fig. 1-16). To this end, the pressure, temperature and composition of the gases in the cylinder are generally assumed to be alterable as a function of time and thus crank angle, yet independent of their location in the cylinder. Consequently, the cylinder charge is considered homogenous. This is referred to as a single zone model. Naturally, this premise does not correspond to the actual processes in a diesel engine cylinder; however, it yields computerized results that are accurate enough for most development

Table 1-4 Differences of different submodels in the ideal and real cycle

Submodel	Ideal cycle	Real cycle
Physical properties	Ideal gas	Real gas; composition changes during the cycle
	c_p, c_v, κ = constant	Physical properties are a function of pressure, temperature and composition
Gas exchange	Gas exchange as heat dissipation	Mass exchange through the valves, residual exhaust gas remains in the cylinder
Combustion	Complete combustion based on specified, idealized regularity	Different combustion characteristics possible depending on mixture formation and combustion cycle; fuel burns partially or incompletely
Wall heat losses	Wall heat losses are ignored	Wall heat losses are factored in
Leaks	Leaks are ignored	Leaks are partially factored in, however ignored in this introduction

work as long as there is no intention to simulate concentrations of pollutants. The formation mechanisms of pollutants, especially nitrogen oxides, are highly dependent on temperature and require the temperature in the burned mixture (post-flame zone) as an input value. It is significantly higher than the energy-averaged temperature of the single zone model. In this case, the cylinder charge is divided into two zones (two zone model [1-24–1-27]). One zone contains the unburned components of fresh air, fuel and residual exhaust gas (relatively low temperature), the other zone the reaction products of exhaust gas and unutilized air (high temperature). Both zones are separated by an infinitesimally small flame front in which the (primary) fuel oxidizes. Figure 1-17 presents both the average temperature of the single zone model and the temperatures of both zones of the two zone model for a diesel engine's high pressure cycle. Clearly, the burned zone has a significantly higher temperature level than in the single zone model. Nonetheless, only the single zone model will be examined to introduce the methods of real cycle simulation.

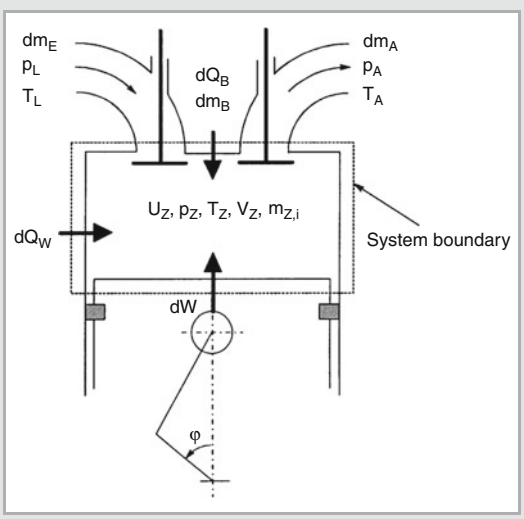

Fig. 1-16 Thermodynamic model of the cylinder

Thermal and Calorific Equations of State

The state of the charge in the cylinder is described by pressure p, temperature T, volume V and composition (masses m_i of the components i). A physical relation exists between these values, the thermal equation of state. In the case of the ideal gas, it is:

$$p \cdot V = m \cdot R \cdot T \tag{1-16}$$

where R is the gas constants and the total mass m is the total of the partial masses of the individual components:

$$m = m_1 + m_2 + \ldots + m_i \tag{1-17}$$

If the cylinder charge is regarded as a real gas, then Eq. (1-16) must be replaced by one of the many equations of state for real gases familiar from the literature (e.g. Justi [1-28], Zacharias [1-29]).

With the aid of the calorific equation of state, the state variables p and T yield the specific internal energy u_i for every component i. In the case of the ideal gas, this is

$$\mathrm{d}u_i(T) = c_{v,i}(T) \cdot dT \tag{1-18}$$

where c_v is the specific isochoric thermal capacity. As a rule, c_v is a function of temperature. In the case of real gases, c_v and thus u is a function of temperature and pressure and can, for example, be taken from appropriate collections of tables or calculated [1-30–1-32, 1-27, 1-29].

Laws of Mass and Energy Conservation

The cylinder contains a charge mass m with a certain composition. The mass can change by being fed in or drawn off through the intake valve $\mathrm{d}m_E$, the exhaust valve $\mathrm{d}m_A$ or the injection valve $\mathrm{d}m_B$. (Gas losses by leaks are disregarded

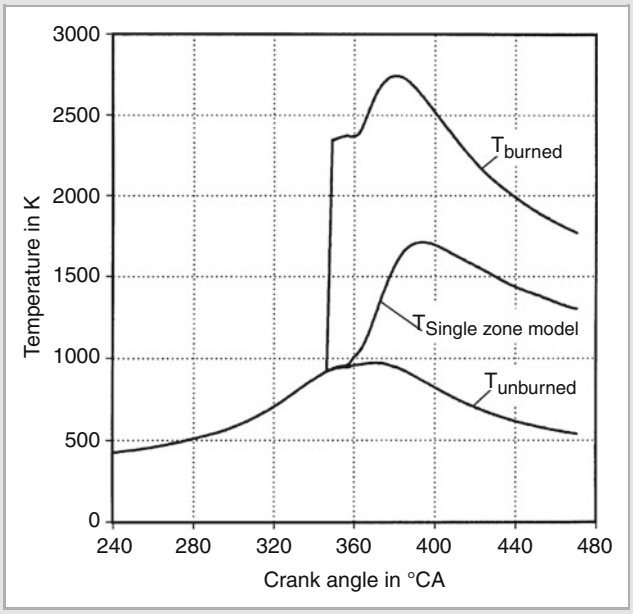

Fig. 1-17
Temperature curves for single and two zone models

here). The law of mass conservation yields the following equation:

$$dm = dm_E + dm_A + dm_B \quad (1\text{-}19)$$

The influent masses are entered positively in Eq. (1-19) and the effluent masses negatively.

The first law of thermodynamics describes the conservation of energy. It states that the energy inside the cylinder U can only change when enthalpy dH is supplied or removed through the system boundary in conjunction with mass dm, heat dQ_W or work (d$W = -p \cdot dV$). The energy released by the combustion of the injected fuel is regarded as internal heat input dQ_B. The law of energy conservation from the first law of thermodynamics describes the correlation between the individual forms of energy:

$$dW + dQ_W + dQ_B + dH_E + dH_A + dH_B = dU \quad (1\text{-}20)$$

When the individual terms of this differential equation are known, then it can be solved with appropriate mathematical methods. The Runge-Kutta method (cf. [1-33]) or algorithms derived from it are usually applied. First, the initial state in the cylinder when "intake closes" is estimated and then Eq. (1-20) is integrated with the algorithm selected for one combustion cycle in small crank angle steps. A check at the end of the combustion cycle to determines whether the estimated initial state is produced when the "intake closes". If this is not the case, improved estimated values are employed to calculate combustion cycles until the estimated values are reproduced with sufficient accuracy.

Wall Heat Losses

Wall heat losses are calculated according to the relationship

$$\frac{dQ_W}{d\varphi} = \frac{1}{\omega} \cdot h \cdot A \cdot (T - T_W) \quad (1\text{-}21)$$

where the angular velocity is $\omega = 2 \cdot \pi \cdot n$, the mean heat transfer coefficient α, the heat transferring area A and the wall temperature T_W. The heat transferring area consists of the areas of the cylinder head, piston crown and cylinder liner enabled for the particular crank angle. Either known from measurements or estimated, an average wall temperature is needed for every area. Since exhaust valves have a significantly higher temperature than the cylinder head, the area of the cylinder head is normally divided into the exhaust valve area and remaining area.

Many authors already deal with calculating the heat transfer coefficient before beginning to simulate the engine process. The equation used most today stems from Woschni [1-34] (see Sect. 7.2 and [1-26, 1-35, 1-27]).

Gas Exchange

The enthalpies of the masses flowing in and out through the intake and exhaust valves are produced from the product of specific enthalpy h and mass change dm:

$$\begin{aligned} dH_E &= h_E \cdot dm_E \\ dH_A &= h_A \cdot dm_A \end{aligned} \quad (1\text{-}22)$$

The specific enthalpies are simulated with the respective temperature before, in or after the cylinder. The following equation yields the mass elements that cross the system boundary [1-26, 1-27]:

$$\frac{\mathrm{d}m_{\mathrm{id}}}{\mathrm{d}\varphi} = \frac{A(\varphi)}{2 \cdot \pi \cdot n} \cdot \frac{p_v}{(R \cdot T_{\mathrm{v}})^{0.5}} \cdot \left\{ \frac{2 \cdot \kappa}{\kappa - 1} \left[\left(\frac{p_{\mathrm{n}}}{p_{\mathrm{v}}} \right)^{2/\kappa} - \left(\frac{p_{\mathrm{n}}}{p_{\mathrm{v}}} \right)^{(\kappa+1)/\kappa} \right] \right\}^{0.5} \tag{1-23}$$

The states "v" and "n" each relate to the conditions before or after the valve analyzed (e.g. to the state of the charge air and the state in the cylinder for an intake valve with normal inflow, i.e. without backflow).

Equation (1.23) is based on the flow equation for the isentropic (frictionless and adiabatic) port flow of ideal gases [1-26, 1-27]. Area A denotes the geometric flow cross-section enabled by the valve at a given instant (see Sect. 2.1).

In real engine operation, frictional losses and spray contraction generate a mass flow that is reduced compared to the ideal value. Defining a standard cross section, this is factored into the flow factors μ determined in experiments on a swirl flow test bench [1-36]. Therefore, the related reference areas must always be known whenever flow factors (also denoted with μ, σ or α) are compared (see Sect. 2.1).

The pressures before the intake valve and after the exhaust valve are needed to calculate the charge flow according to Eq. (1-23). In the case of an exhaust gas turbocharged engine, boost pressure und exhaust gas pressure before the turbine are produced by balancing the exhaust gas turbocharger with the aid of measured compressor and turbine maps (see Sect. 1.3.2).

Combustion Characteristic

In addition to the physical models treated thus far, a description of combustion is required to model a cylinder. The energy released by combustion is produced by the specific calorific value H_{u} and the unburned fuel mass $\mathrm{d}m_{\mathrm{B}}$:

$$\mathrm{d}Q_{\mathrm{B}} = H_{\mathrm{u}} \cdot \mathrm{d}m_{\mathrm{B}} \tag{1-24}$$

while disregarding the enthalpy of the injected fuel $\mathrm{d}H_{\mathrm{B}}$.

A function of time or the crank angle, the curve of the energy released by combustion (combustion characteristic $\mathrm{d}Q_{\mathrm{B}}/\mathrm{d}\varphi$) is one of the most important set parameters for engine process simulation. In contrast to ideal cycles (Sect. 1.2) in which the combustion characteristic directly results from the desired pressure curve (e.g. constant pressure or constant volume cycle), a real engine's combustion characteristic depends on many parameters.

An approach that follows Fig. 1-18 would be optimal: The injection pump's delivery curve is the sole set parameter. The injection system (injection pump, rail and nozzle) is then simulated with suitable models to calculate the injection characteristic from the delivery curve. If there were sufficient knowledge of the physical processes during spray disintegration, evaporation and mixture formation, it would be possible to simulate the ignition delay and combustion (combustion characteristic) with mathematical models [1-37, 1-38].

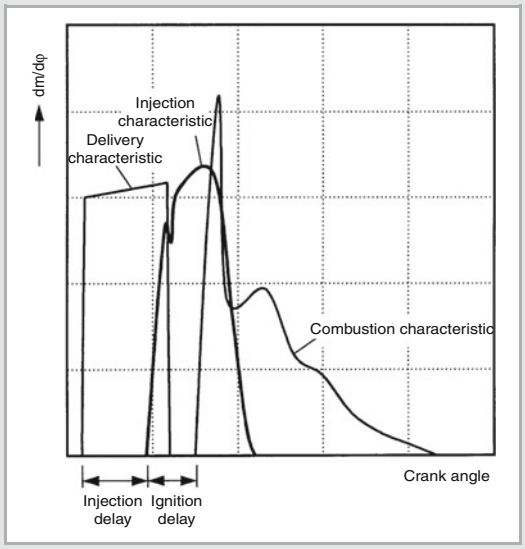

Fig. 1-18 Delivery curve, injection characteristic and combustion characteristic

However, the models and methods developed so far are not yet able to predetermine diesel engine combustion with the accuracy desired to simulate the engine process. Knowledge about the combustion processes in internal combustion engines mostly comes from cylinder pressure indication. These measurements supply information on the processes inside a cylinder, piezoelectric pressure gauges being applied when the resolution is high, e.g. every 0.5°CA or less [1-39–1-41]. When the cylinder pressure curve is known, the combustion characteristic can be determined by inverting Eq. (1-18) (pressure curve analysis). This delivers insight into the conversion of energy in the engine.

Instead of the combustion characteristic calculated from the pressure curve analysis, a simple mathematical function, the rate of heat release, is usually employed to simulate the engine process. Optimization methods can be applied to select this function's parameters so that the combustion characteristic known from the pressure curve analysis is optimally reproduced. If cylinder pressure indication is unavailable, measured engines are simulated on a test bench with the aid of engine process simulation and a selected rate of heat release is estimated so that the measured and calculated parameters concur.

The most commonly applied rate of heat release goes back to the work of Vibe [1-42] who uses an exponential

function to specify the integral of the rate of heat release (total combustion characteristic or combustion function $Q_B(\varphi)$):

$$\frac{Q_B(\varphi)}{Q_{B,O}} = 1 - \exp\left[-6.908 \cdot \left(\frac{\varphi - \varphi_{VB}}{\varphi_{VE} - \varphi_{VB}}\right)^{m+1}\right] \quad (1\text{-}25)$$

φ_{VB}: start of combustion
φ_{VE}: end of combustion
$Q_{B,0}$: total energy $Q_B(\varphi_{VE})$ released at the end of combustion
m: form factor.

The factor −6.908 is produced by calibrating the asymptotic exponential function moving toward zero to a numerical value of 0.001 at the end of combustion.

The rate of heat release $dQ_B/d\varphi$ is obtained as a derivative of Eq. (1-25):

$$\frac{dQ_B}{d\varphi} = \frac{Q_{B,0}}{\varphi_{VE} - \varphi_{VB}} \cdot 6.908 \cdot (m+1) \cdot \left(\frac{\varphi - \varphi_{VB}}{\varphi_{VE} - \varphi_{VB}}\right)^{m} \cdot \exp\left[-6.908 \cdot \left(\frac{\varphi - \varphi_{VB}}{\varphi_{VE} - \varphi_{VB}}\right)^{m+1}\right] \quad (1\text{-}26)$$

An equation called the Vibe function describes combustion with three parameters: the start of combustion φ_{VB}, the duration of combustion $\Delta\varphi_{BD} = \varphi_{VE} - \varphi_{VB}$ and the form factor m. As can be gathered from Fig. 1-19, the form factor defines the relative position of the maximum of the Vibe function.

One important task of engine process simulation is to ascertain the influence of changed boundary conditions, e.g. ambient conditions, on the combustion cycle in parameter studies (Sects. 1.3.3.3 and 1.3.3.4). The prerequisite for such simulation is knowledge of the influence of significant engine parameters on the rate of heat release as boundary conditions.

Woschni/Anisits [1-43] calculated the following dependencies of the air/fuel ratio λ, conversion factor η_u, speed n and state during "intake closed" (index IC) for the Vibe function:

$$\frac{\Delta\varphi_{BD}}{\Delta\varphi_{BD,0}} = \left(\frac{\lambda_V}{\lambda_{V,0}}\right)^{-0.6} \cdot \left(\frac{n}{n_0}\right)^{0.5} \cdot \eta_u^{0.6} \quad (1\text{-}27)$$

$$\frac{m}{m_0} = \left(\frac{\Delta\varphi_{BD}}{\Delta\varphi_{BD,0}}\right)^{-0.5} \cdot \frac{p_{Es}}{p_{Es,0}} \cdot \frac{T_{Es}}{T_{Es,0}} \left(\frac{n}{n_0}\right)^{-0.3} \quad (1\text{-}28)$$

Index 0 refers to the known initial operating point.

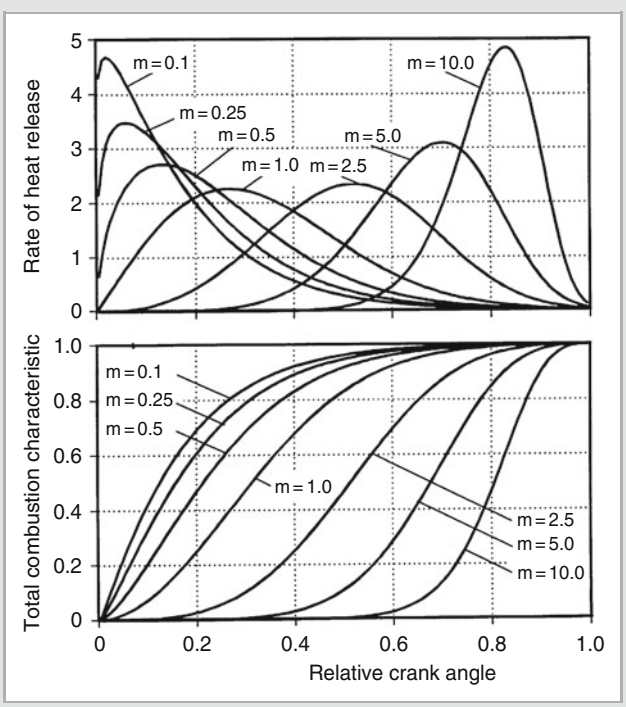

Fig. 1-19
Vibe function for different form factors (m)

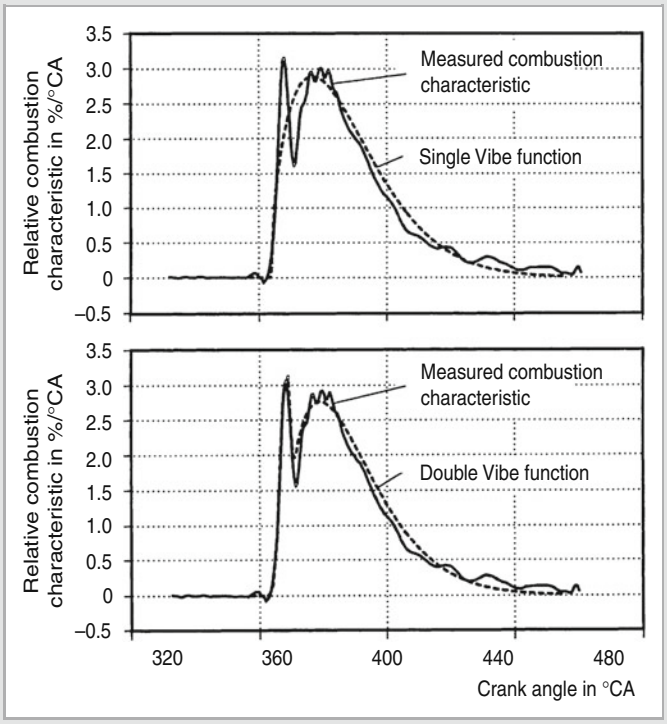

Fig. 1-20
Approximation of a combustion characteristic by the double Vibe function

The start of combustion ensues from the start of delivery φ_{FB}, the injection delay $\Delta\varphi_{EV}$ and the ignition delay $\Delta\varphi_{ZV}$:

$$\frac{\Delta\varphi_{EV}}{\Delta\varphi_{EV,0}} = \frac{n}{n_0} \tag{1-29}$$

$$\frac{\Delta\varphi_{ZV}}{\Delta\varphi_{ZV,0}} = \frac{n}{n_0} \cdot \frac{\exp\left(\frac{b}{Tzv}\right)}{\exp\left(\frac{b}{T_{zv,0}}\right)} \cdot \left(\frac{p_{ZV}}{p_{ZV,0}}\right)^{-c} \tag{1-30}$$

p_{ZV}: pressure in the ignition delay phase
T_{ZV}: temperature in the ignition delay phase
b, c: from parameters of the equation that have to be determined from measurements.

Other approaches to ignition delay can be found in [1-44–1-46].

Since its simple mathematical form prevents the Vibe function from reproducing combustion characteristics with sufficient accuracy, especially for high speed direct injection diesel engines, two Vibe functions are sometimes combined as a "double Vibe function" [1-47]. Figure 1-20 presents an operating point for a high performance high speed diesel engine reproduced by the Vibe function and the double Vibe function. Clearly, the simple Vibe function (Eq. (1-29)) cannot describe the rise of the combustion characteristic at the start of combustion ("premixed peak").

1.3.2.2 Indicated and Effective Work

The solution to the differential equation Eq. (1-20) for the first law of thermodynamics delivers the pressure curve in the cylinder and thus the indicated work W_i from which the mean indicated pressure p_i and the specific indicated work w_i can be derived as engine parameters (see Sect. 1.2). However, in general, the so-called brake mean effective pressure p_e and the specific effective work w_e are usually of interest. Hence when simulating the real cycle, model statements are used to simulate frictional losses expressed by the mean friction pressure p_r as the difference of p_i and p_e ($p_r = p_i - p_e$) if unknown from measurements.

The literature contains various suggestions for calculating frictional work [1-38, 1-48, 1-49], which, depending on the author, may be a function of speed, load, engine geometry, boost pressure and water and oil temperatures. Starting from the friction pressure (index 0 in Eq. (1-31)) determined in a design point according to [1-38] for example, the following applies

$$\frac{p_r - p_{r,0}}{p_{r,0}} = 0.7 \cdot \frac{n - n_0}{n_0} + 0.3 \cdot \frac{p_i - p_{i,0}}{p_{i,0}} \tag{1-31}$$

according to which only speed and mean indicated pressure have to be specified.

1.3.2.3 Modeling the Complete Engine

A cylinder was modeled as an example in Sects. 1.3.2.1 and 1.3.2.2. Naturally, every significant engine component must be modeled to simulate a complete engine. Likewise, the basic physical equations of mass conservation (continuity equation), impulse (conservation of impulse) and energy (first law of thermodynamics) as well as the second law of thermodynamics must be solved for every flow process outside the cylinder in such engine components as the intake and exhaust manifolds, intercooler, catalytic converter or exhaust gas turbocharger. The first simulations of this type were performed with the program system PROMO [1-50, 1-51]. Commercial programs such as GT-Power (a component of the GT-Suite [1-52]) or Boost (from AVL [1-53]) are generally used today.

Various methods, which also describe real conditions more accurately as complexity increases, lend themselves to the simulation of air and exhaust manifolds. In the simplest case, pressures in the charge air and exhaust manifolds (i.e. infinitely large reservoirs) are assumed to be constant (so-called zero dimensional models). The so-called filling and emptying method models the manifolds as reservoirs of finite volume, which are transiently filled and emptied by the cylinders and continuously filled and emptied by the supercharger or the turbine. In this method, the pressure in the manifolds varies temporally but not locally (i.e. the sound of speed is infinitely great).

When the equations are employed for nonstationary, one-dimensional and compressible pipe flow, the changes of state in the intake and exhaust system are captured with the methods of transient gas dynamics (characteristic method or simplifying acoustic method [1-54]). This one-dimensional method can also simulate local pressure differences and pipe branches, the mathematical work required being far greater than the filling and emptying method.

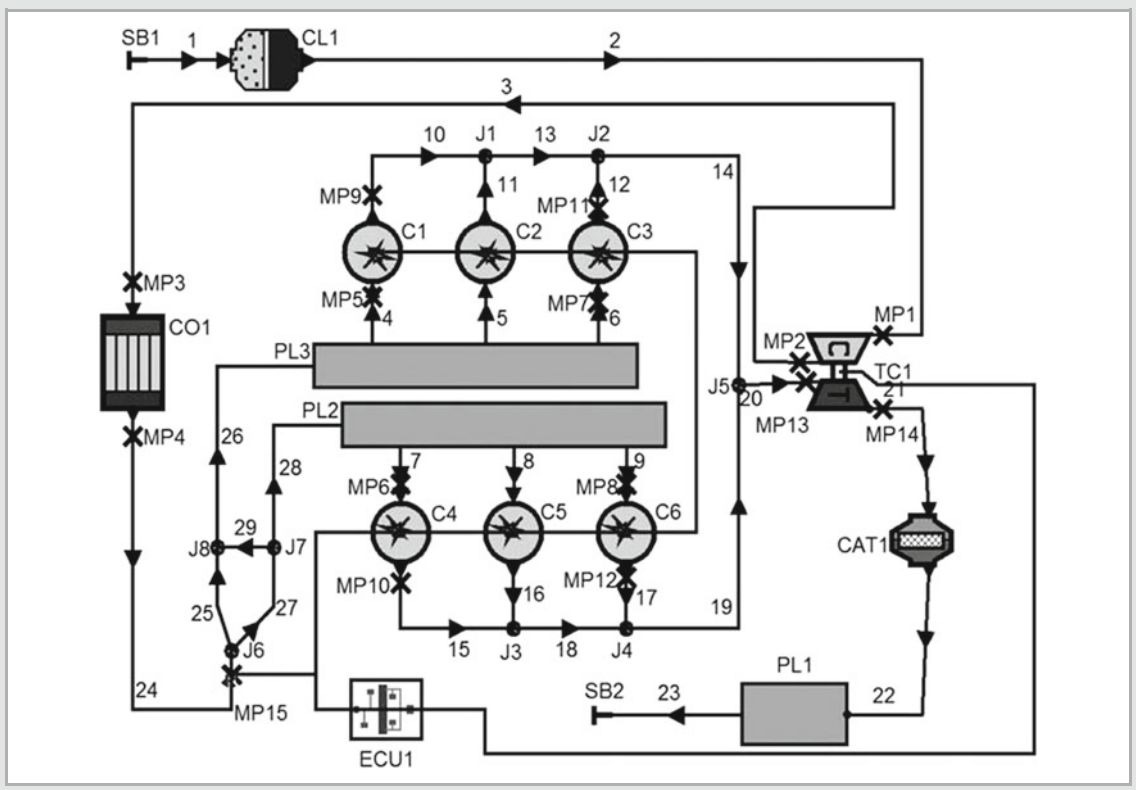

Fig. 1-21 Model for simulating a supercharged V6 diesel engine: (CL1) air filter, (TC1) exhaust gas turbocharger, (C01) intercooler, (CAT1) catalytic converter, (PL1) muffler, (PL2, PL3) V engine intake manifold, (C1 to C6) engine cylinders, (J) connections and branches, (ECU1) engine electronics to control injection and the turbocharger's wastegate [1-39]

More recently, quasidimensional models have been developed in which variables that are a function of position and time factor in local phenomena. Examples include flow cycle, combustion and heat transfer models [1-27].

Figure 1-21 presents a model of an exhaust gas turbocharged six cylinder diesel engine simulated with the Boost program as an example [1-53]. It incorporates all the significant components attached to the engine, beginning with the air filter to the exhaust gas turbocharger up through the catalytic converter and exhaust muffler. The modeled engine electronics (ECU1), which controls injection and the turbocharger's wastegate, is added to this.

So as not to prolong this introduction to engine process simulation, the authors refer readers to further literature (e.g. [1-26, 1-27] or [1-55, 1-56]) and Sect. 2.2.

1.3.3 Typical Examples of the Application of Engine Process Simulation

1.3.3.1 Introduction

Basically, two types of application are distinguished:

1. Measured data is already available for the engine operating point being simulated.

   In this case, engine process simulation determines parameters that are already known from measurement. Comparing the computed and measured results allows checking the plausibility of the measured results for instance or computing the physical submodels of the process simulation (e.g. rate of heat release, wall heat transfer and mean effective friction pressure).
2. Measured data is not yet available for the engine operating point being simulated.

   In this case, the engine process simulation is a projection of a yet unknown operating point. First, the parameters of the physical submodels must be estimated, i.e. they are adopted from a similar operating point and, if necessary, corrected with the conversion equations specified in Sects. 1.3.2.2 and 1.3.2.3. Naturally, the results of this process simulation are only as precise as the relationships used for the conversion. Therefore, in practice, they are checked and calibrated for the particular engines by resimulating as many measured operating points as possible with the engine process simulation and comparing the results with the measured values.

Thus, the difference between a process simulation to design new engines and a resimulation of already measured engines is insubstantial.

1.3.3.2 Results of Engine Process Simulation

Based on Sect. 1.3.2, typical input variables for engine process simulation are:

Engine geometry, valve lift curve, valve flow coefficients, speed, engine power, mechanical efficiency, rate of heat release, coefficients for the heat transfer equation, component wall temperatures, charge air pressure and temperature before the cylinder and pressure after the cylinder.

Typical Results Are

Pressure curve, temperature curve, wall heat losses, effective fuel consumption, net efficiency, internal efficiency, maximum combustion pressure, maximum final compression pressure, maximum rate of pressure rise, maximum cycle temperature (average energy value), temperature before the exhaust gas turbine, gas exchange losses, charge flow and the air/fuel ratio.

When, in addition to the cylinder, the exhaust gas turbocharger can also be described thermodynamically as well, e.g. by employing appropriate compressor and turbine maps, then the engine process simulation ascertains the pressure before and after the cylinder. Then, the ambient condition counts as an input variable. If the potentially present intercooler is also modeled in the further course of process simulation, then, when the ambient temperature is given, the engine process simulation also yields the charge air temperature in addition to the water temperature when the charge air is water cooled.

As an example, Fig. 1-22 presents the results of a process simulation of an engine with a cylinder displacement of 4 dm^3 and a specific effective work w_e of 2 kJ/dm^3 for the operating point $n = 1{,}500/min$. It represents pressure, temperature, combustion characteristic, mass flow in the cylinder and valves as well as the wall heat losses as a function of the crank angle. The correspondence between the engine process simulation and reality is verified by comparing global values, e.g. exhaust gas temperature, charge flow or boost pressure, with measured values. When they correspond, it is assumed that even the unverifiable values such as temperature curve or mass curve have been simulated correctly.

1.3.3.3 Parameter Studies

A significant field of application for engine process simulation is parameter studies that analyze the influence of boundary conditions on the combustion cycle in depth. The results are needed in the design phase of new engines or to optimize or enhance the performance of existing engines. Parameter studies may have optimum fuel consumption, power and torque values as possible target parameters. Optimizations may be implemented so that engineering or legal limits for maximum combustion pressure, rate of pressure increase, exhaust gas temperature or pollutant emissions are not exceeded.

The outcome of a typical parameter study is presented below. Since the maximum combustion pressure limited

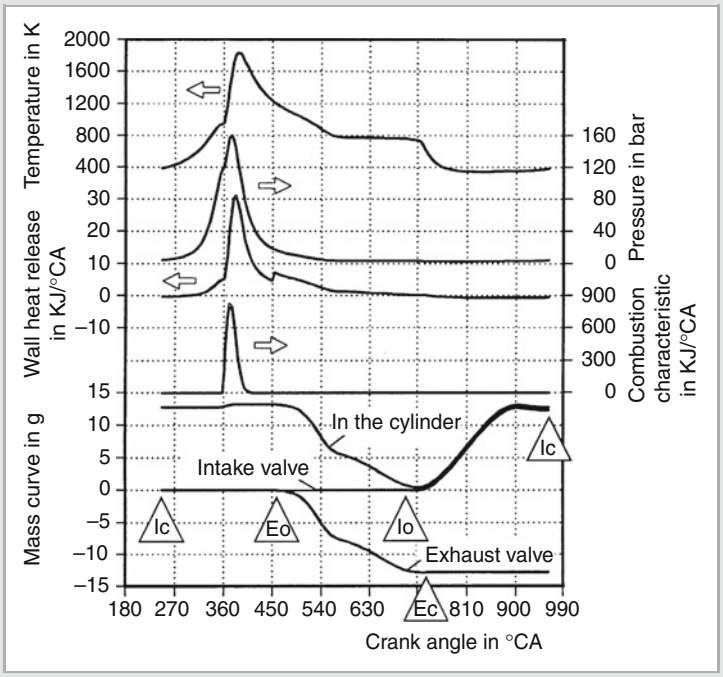

Fig. 1-22
Results of the engine process simulation

by engineering greatly influences a cycle's net efficiency and thus its fuel consumption, one of the most important parameter studies serves to determine the dependence of net efficiency η_e on maximum combustion pressure p_{Zmax}. When the combustion characteristic is given, the maximum combustion pressure is defined by the parameters of start of delivery (and thus start of combustion) and final compression pressure. The latter, in turn, primarily depends on the compression ratio and the boost pressure. The boost pressure is itself essentially defined by the exhaust gas turbocharging efficiency and the desired air/fuel ratio. Figure 1-23 presents the net efficiency η_e as a function of the compression ratio ε for various maximum combustion pressures at constant numerical values for the exhaust gas turbocharging efficiency η_{TL} and the air/fuel ratio λ. The dotted lines indicate the position of the start of combustion. An optimum compression ratio with a maximum efficiency η_e exists for every maximum combustion pressure. (By contrast, theoretical standard cycles state that maximum net efficiency is attained at the maximum compression ratio.)

1.3.3.4 Other Examples of Application

Apart from parameter studies, engine process simulation also serves many other purposes.

- heat balance, loss analysis: simulation of heat balances and analyses of losses to assess engines (development potential, optimization, cooling system design)
- design of exhaust gas turbocharging groups: simulation of the energy supply available for supercharging (exhaust gas mass flow and temperature) and the boost pressure requirement and air flow rate [1-57]
- optimization of valve lift and valve gear timing: simulation of the gas exchange with the goal of low gas exchange losses and large volumetric efficiencies
- temperature field simulation: simulation of engines' heat balance and thermal load (input variables for simulating the temperature fields in the cylinder, cylinder liner, piston and valves) (see Sect. 7.1)
- gas pressure curves for further studies: simulation of the gas pressure curves as input variables for further studies such as strength simulation, torsional vibration analysis, piston ring movement simulation
- wet corrosion: analysis of the danger of wet corrosion (undershooting of the exhaust gas dew-point temperature)
- nitrogen oxide emissions: application of a combustion model (e.g. two zone model) to analyze nitrogen oxide emissions [1-24–1-27]
- ambient conditions: determination of engines' operating values when ambient conditions (pressure and temperature) change

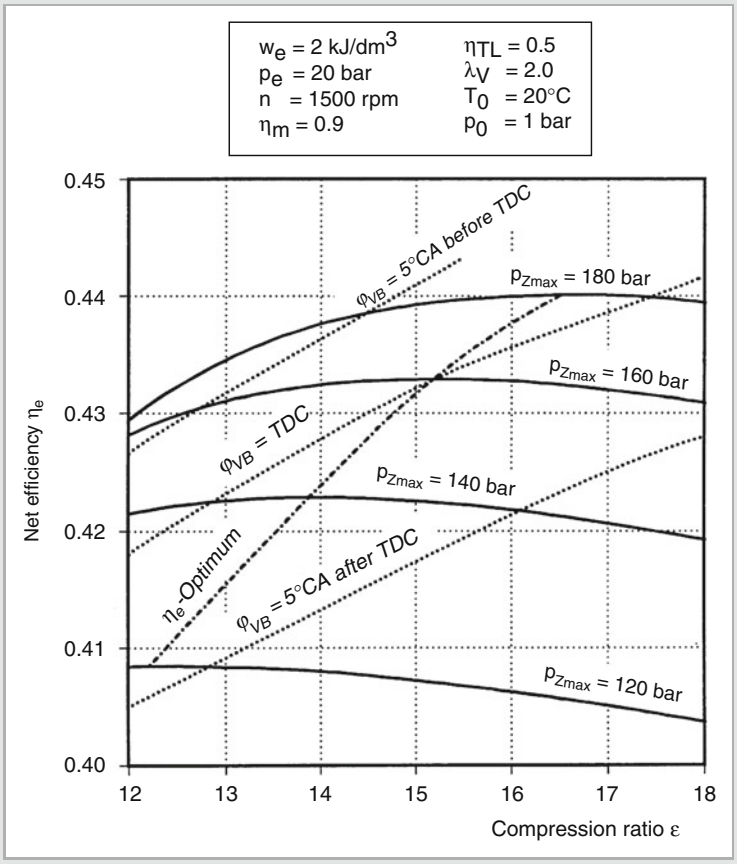

Fig. 1-23
Dependence of net efficiency η_e on the compression ratio ε and the maximum combustion pressure p_{Zmax}

– plausibility check: plausibility check of measured values or hypotheses for a damage analysis
– transfer of experimental single cylinder results to multi-cylinder engines: conversion of the operating values measured in an experimental single cylinder engine to conditions for multi-cylinder engines.

1.3.4 Future Studies/Work in the Field of Engine Process Simulation

Engine process simulation is an instrument suitable for relative statements (e.g. parameter studies). The requirements for submodel accuracy are not as great. Absolute statements (e.g. supercharger or cooling systems design, comparisons of different engines) require far more accurate submodels. Therefore, many and diverse efforts are being made to further improve the models.

When maximum combustion pressures are elevated above 200 bar, the cylinder charge may no longer be considered an ideal gas and the real gas properties of the components involved have to be factored in [1-29].

Present heat transfer models calculate wall heat losses in the part load region too small. Furthermore, they only allow for heat losses radiating from soot particulates during combustion imprecisely or not at all. Consequently, the calculated losses are too small, especially when combustion is poor. Pressure curve analysis yields apparent energy losses in the compression phase, which may be due to inaccuracies in the dependence of the crank angle in the wall heat models employed. New heat transfer models may be found in [1-58–1-63].

Simulation of the charge flow can be improved by applying computationally very intensive simulations of three-dimensional flow fields. Such simulations enable optimizing flow conditions in cylinder heads for example. Flow field simulations may also be applied to analyze mixture formation and in part to already simulate the combustion cycle [1-26, 1-27].

Work is being done on simulating the combustion characteristic directly from injection data [1-64, 1-65, 1-37, 1-38, 1-24, 1-66, 1-67]. On the other hand, the models of the rate of heat release and its conversion in

the map have to be improved [1-68] in order to be able to describe combustion with better precision when simulating nitrogen oxide emissions [1-24].

Other studies also being performed on converting the mean effective friction pressure in the map are aimed at determining the individual assemblies' contribution to the total frictional losses [1-48].

Literature

1-1 DRP Nr. 67207: Arbeitsverfahren und Ausführungsart für Verbrennungskraftmaschinen. To: R. Diesel as of February 28, 1892

1-2 Diesel, R.: Die Entstehung des Dieselmotors. Berlin/Heidelberg/New York: Springer (1913)

1-3 Diesel, R.: Theorie und Konstruktion eines rationellen Wärmemotors zum Ersatz der Dampfmaschinen und der heute bekannten Verbrennungsmotoren. Berlin/Heidelberg/New York: Springer (1893), Reprint: Düsseldorf: VDI-Verlag (1986)

1-4 Sass, F.: Geschichte des deutschen Verbrennungsmotorenbaus von 1860–1918. Berlin/Göttingen/Heidelberg: Springer (1962)

1-5 Reuss, H.-J.: Hundert Jahre Dieselmotor. Stuttgart: Franckh-Kosmos (1993)

1-6 Adolf, P.: Die Entwicklung des Kohlenstaubmotors in Deutschland. Diss. TU Berlin (D83) (1992)

1-7 Knie, A.: Diesel – Karriere einer Technik: Genese und Formierungsprozesse im Motorenbau. Berlin: Bohn (1991)

1-8 Heinisch, R.: Leichter, komfortabler, produktiver – die technologische Renaissance der Bahn. Mobil 1 (1994) 3. Also: Heinrich, J.: Flinker CargoSprinter hilft der Deutschen Bahn. VDInachr. (1996) 41, pp. 89 ff.

1-9 Diesel, E.: Die Geschichte des Diesel-Personenwagens. Stuttgart: Reclam (1955)

1-10 Diesel, E.: Diesel. Der Mensch, das Werk, das Schicksal. Stuttgart: Reclam (1953)

1-11 Boie, W.: Vom Brennstoff zum Rauchgas. Leipzig: Teubner (1957)

1-12 Schmidt, E.: Einführung in die technische Thermodynamik. 10th Ed. Berlin/Heidelberg/New York: Springer (1963)

1-13 Pflaum, W.: I, S-Diagramme für Verbrennungsgase, 2nd Ed. Part I and II. Düsseldorf: VDI-Verlag (1960, 1974)

1-14 DIN ISO 3046/1: Reciprocating internal combustion engines – Performance – Part 1: Declarations of power, fuel and lubricating oil consumptions, and test methods

1-15 Technical Review Wärtsilä RT-flex 96C / Wärtsilä RTA 96C. Wärtsilä Corporation publication (2006)

1-16 Steinparzer, F.; Kratochwill, H.; Mattes, T.; Steinmayr, T.: Der neue Sechszylinder-Dieselmotor von BMW mit zweistufiger Abgasturboaufladung – Spitzenstellung bezüglich effizienter Dynamik im Dieselsegment. Proceedings of the 15th Aachen Colloquium Automobile and Engine Technology 2006, pp. 1281–1301

1-17 Groth, K.; Syassen, O.: Dieselmotoren der letzten 50 Jahre im Spiegel der MTZ – Höhepunkte und Besonderheiten der Entwicklung. MTZ 50 (1989) pp. 301–312

1-18 Woschni, G.: Elektronische Berechnung von Verbrennungsmotor-Kreisprozessen. MTZ 26 (1965) 11, pp. 439–446

1-19 Woschni, G.: CIMAC Working Group Supercharging: Programmiertes Berechnungsverfahren zur Bestimmung der Prozessdaten aufgeladener Vier- und Zweitaktdieselmotoren bei geänderten Betriebsbedingungen. TU Braunschweig. Forschungsvereinigung Verbrennungskraftmaschinen e.V. (FVV) Frankfurt (1974)

1-20 Albers, W.: Beitrag zur Optimierung eines direkteinspritzenden Dieselmotors durch Variation von Verdichtungsverhältnis und Ladedruck. Diss. Universität Hannover (1983)

1-21 Schorn, N.: Beitrag zur rechnerischen Untersuchung des Instationärverhaltens abgasturboaufgeladener Fahrzeugdieselmotoren. Diss. RWTH Aachen (1986)

1-22 Zellbeck, H.: Rechnerische Untersuchung des dynamischen Betriebsverhaltens aufgeladener Dieselmotoren. Diss. TU München (1981)

1-23 Friedrich, I.; Pucher, H.; Roesler, C.: Echtzeit-DVA – Grundlage der Regelung künftiger Verbrennungsmotoren. MTZ-Konferenz-Motor Der Antrieb von Morgen. Wiesbaden: GWV Fachverlage 2006, pp. 215–223

1-24 Hohlbaum, B.: Beitrag zur rechnerischen Untersuchung der Stickstoffoxid-Bildung schnellaufender Hochleistungsdieselmotoren. Diss. Universität Karlsruhe (TH) (1992)

1-25 Krassnig, G.: Die Berechnung der Stickoxidbildung im Dieselmotor. Habilitation TU Graz (1976)

1-26 Merker, G.; Schwarz, C.; Stiesch, G.; Otto, F.: Verbrennungsmotoren: Simulation der Verbrennung und Schadstoffbildung. Wiesbaden: Teubner-Verlag (2004)

1-27 Pischinger, R.; Klell, M.; Sams, T.: Thermodynamik der Verbrennungskraftmaschine – Der Fahrzeugantrieb. Wien: Springer (2002)

1-28 Justi, E.: Spezifische Wärme, Enthalpie, Entropie und Dissoziation technischer Gase. Berlin: Springer (1938)

1-29 Zacharias, F.: Analytische Darstellung der thermodynamischen Eigenschaften von Verbrennungsgasen. Diss. Berlin (1966)

1-30 Heywood, J.B.: Internal Combustion Engine Fundamentals. New York: McGraw-Hill Book Company (1988)

1-31 NIST/JANAF: Thermochemical Tables Database. Version 1.0 (1993)

1-32 Pflaum, W.: Mollier-(I, S-)Diagramme für Verbrennungsgase, Teil II. Düsseldorf: VDI-Verlag (1974)

1-33 Zurmühl, R.: Praktische Mathematik für Ingenieure und Physiker. Berlin/Heidelberg/New York: Springer (1984)
1-34 Woschni, G.: Die Berechnung der Wandverluste und der thermischen Belastung der Bauteile von Dieselmotoren. MTZ 31 (1970) 12, pp. 491–499
1-35 Pflaum, W.; Mollenhauer, K.: Wärmeübergang in der Verbrennungskraftmaschine. Vienna: Springer (1977)
1-36 Frank, W.: Beschreibung von Einlasskanaldrallströmungen für 4-Takt-Hubkolbenmotoren auf Grundlage stationärer Durchströmversuche. Diss. RWTH Aachen (1985)
1-37 Constien, M.; Woschni, G.: Vorausberechnung des Brennverlaufs aus dem Einspritzverlauf für einen direkteinspritzenden Dieselmotor. MTZ 53 (1992) 7/8, pp. 340–346
1-38 Flenker, H.; Woschni, G.: Vergleich berechneter und gemessener Betriebsergebnisse aufgeladener Viertakt-Dieselmotoren. MTZ 40 (1979) 1, pp. 37–40
1-39 Hohenberg, G.; Möllers, M.: Zylinderdruckindizierung I. Abschlussbericht Vorhaben No. 362. Forschungsvereinigung Verbrennungskraftmaschinen (1986)
1-40 Nitzschke, E.; Köhler, D.; Schmidt, C.: Zylinderdruckindizierung II. Abschlussbericht Vorhaben Nr. 392. Forschungsvereinigung Verbrennungskraftmaschinen (1989)
1-41 Thiemann, W.: Verfahren zur genauen Zylinderdruckmessung an Verbrennungsmotoren. Part 1: MTZ 50 (1989), Vol. 2, pp. 81–88; Part 2: MTZ 50 (1989) 3, pp. 129–134
1-42 Vibe, I.I.: Brennverlauf und Kreisprozess von Verbrennungsmotoren. Berlin: VEB Verlag Technik (1970)
1-43 Woschni, G.; Anisits, F.: Eine Methode zur Vorausberechnung der Änderung des Brennverlaufs mittelschnellaufender Dieselmotoren bei geänderten Randbedingungen. MTZ 34 (1973) 4, pp. 106–115
1-44 Hardenberg, H.; Wagner, W.: Der Zündverzug in direkteinspritzenden Dieselmotoren. MTZ 32 (1971) 7, pp. 240–248
1-45 Sitkei, G.: Kraftstoffaufbereitung und Verbrennung bei Dieselmotoren. Berlin/Göttingen/Heidelberg: Springer (1964)
1-46 Wolfer, H.: Der Zündverzug im Dieselmotor. VDI Forschungsarbeiten 392. Berlin: VDI Verlag GmbH (1938)
1-47 Oberg, H.J.: Die Darstellung des Brennverlaufs eines schnellaufenden Dieselmotors durch zwei überlagerte Vibe-Funktionen. Diss. TU Braunschweig (1976)
1-48 Schwarzmeier, M.: Der Einfluss des Arbeitsprozessverlaufs auf den Reibmitteldruck. Diss. TU München (1992)
1-49 Thiele, E.: Ermittlung der Reibungsverluste in Verbrennungsmotoren. MTZ 43 (1982) 6, pp. 253–258
1-50 Seifert, H.: Erfahrungen mit einem mathematischen Modell zur Simulation von Arbeitsverfahren in Verbrennungsmotoren. Part 1: MTZ 39 (1978) 7/8, pp. 321–325; Part 2: MTZ 39 (1978) 12, pp. 567–572
1-51 Seifert, H.: 20 Jahre erfolgreiche Entwicklung des Programmsystems PROMO. MTZ 51 (1990) 11, pp. 478–488
1-52 Simulation program GT-Power: www.gtisoft.com
1-53 Simulation program Boost: www.avl.com
1-54 Seifert, H.: Instationäre Strömungsvorgänge in Rohrleitungen an Verbrennungskraftmaschinen. Berlin/Heidelberg/New York: Springer (1962)
1-55 Hiereth, H.; Prenninger, P.: Aufladung der Verbrennungskraftmaschine – Der Fahrzeugantrieb. Vienna: Springer (2003)
1-56 Zinner, K.: Aufladung von Verbrennungsmotoren. Berlin/Heidelberg/New York: Springer (1985)
1-57 Golloch, R.: Downsizing bei Verbrennungsmotoren. Berlin/Heidelberg/New York: Springer 2005
1-58 Bargende, M.: Ein Gleichungsansatz zur Berechnung der instationären Wandwärmeverluste im Hochdruckteil von Ottomotoren. Diss. TH Darmstadt (1991)
1-59 Boulouchos, K.; Eberle, M.; Ineichen, B.; Klukowski, C.: New Insights into the Mechanism of In Cylinder Heat Transfer in Diesel Engines. SAE Congress February 27–March 3, (1989)
1-60 Huber, K.: Der Wärmeübergang schnellaufender, direkteinspritzender Dieselmotoren. Diss. TU München (1990)
1-61 Kleinschmidt, W.: Entwicklung einer Wärmeübergangsformel für schnellaufende Dieselmotoren mit direkter Einspritzung. Zwischenbericht zum DFG Vorhaben K1 600/1 1 (1991)
1-62 Kolesa, K.: Einfluss hoher Wandtemperaturen auf das Betriebsverhalten und insbesondere auf den Wärmeübergang direkteinspritzender Dieselmotoren. Diss. TU München (1987)
1-63 Vogel, C.; Woschni, G.; Zeilinger, K.: Einfluss von Wandablagerungen auf den Wärmeübergang im Verbrennungsmotor. MTZ 55 (1994) 4, pp. 244–247
1-64 Barba, C.; Burckhardt, C.; Boulouchos, K.; Bargende, M.: Empirisches Modell zur Vorausberechnung des Brennverlaufs bei Common-Rail-Dieselmotoren. MTZ 60 (1999) 4, pp. 262–270
1-65 Chemla, F.; Orthaber, G.; Schuster, W.: Die Vorausberechnung des Brennverlaufs von direkteinspritzenden Dieselmotoren auf der Basis des Einspritzverlaufs. MTZ 59 (1998) 7/8
1-66 Witt, A.: Analyse der thermodynamischen Verluste eines Ottomotors unter den Randbedingungen variabler Steuerzeiten. Diss. TU Graz (1999)
1-67 De Neef, A.T.: Untersuchung der Voreinspritzung am schnellaufenden direkteinspritzenden Dieselmotor. Diss. ETH Zürich (1987)
1-68 Schreiner, K.: Untersuchungen zum Ersatzbrennverlauf und Wärmeübergang bei schnellaufenden Hochleistungsdieselmotoren. MTZ 54 (1993) 11, pp. 554–563